



Experimental and numerical investigation of hysteretic earthquake behavior of masonry infilled RC frames with opening strengthened by adding rebar-reinforced stucco

Hamide Tekeli¹ · Ceyhan Yüksel¹ · Özgür Anıl² · Erkan Okay Mutlu³

Received: 10 August 2023 / Accepted: 24 March 2024
© The Author(s) 2024

Abstract

Adding a reinforced stucco layer to the masonry infill walls is a preferred method for strengthening RC frame system structures with an easy-to-apply method that does not require a long time, is economical, and does not require detailed and extensive workmanship. However, no research has been discovered as a result of the extensive literature review that investigates the effects of masonry-infilled RC frames strengthened with a reinforced stucco layer on the seismic performance of openings that must be due to architectural requirements such as doors, windows, installations, and similar ventilation systems. As a result, an experimental study was planned to investigate the effects of the dimensions and location of the opening in the masonry infill walls on the performance of the strengthening method with the reinforced stucco layer. The applied strengthening method increased the ultimate load capacity, initial stiffness, and energy dissipation capacity values of reinforced concrete frames with masonry infill walls by 83%, 226%, and 62%, respectively, but resulted in a 38% decrease in displacement-ductility ratios. The study found that the openings in the masonry infill walls harm the performance of the strengthening technique by adding a rebar-reinforced stucco layer and decreasing the success level. When the opening size increased, and the opening was located at the corner of the masonry wall, the performance of the applied strengthening technique was negatively affected and decreased. Furthermore, nonlinear numerical analyses of the experiments conducted as part of the study were performed using ABAQUS finite element software. The numerical analysis results were compared to the experimental results. It has been determined whether numerical analysis models are compatible with experimental results.

Keywords Masonry infilled RC frames · Rebar-reinforced stucco · Strengthening · Opening

✉ Özgür Anıl
oanil@gazi.edu.tr

¹ Department of Civil Engineering, Süleyman Demirel University, Isparta, Turkey

² Department of Civil Engineering, Gazi University, Ankara, Turkey

³ Department of Civil Engineering, Kırıkkale University, Kırıkkale, Turkey

1 Introduction

In examinations conducted following major earthquakes in seismically active areas, it was observed that structures with RC frame-bearing systems are insufficiently ductile and cannot consume energy in the case of heavy damage and global structural failure. Strengthening the bearing system has often been necessary to increase the seismic performance levels of the existing structural systems, limit the story drift ratios on a system basis, and improve the bearing capacity and rigidity at the structural level. Strengthening masonry infill walls within the portal frame strengthens existing reinforced concrete (RC) frame system structures. In addition to these problems, it has been observed that due to the inability to limit the story drift ratios due to their insufficient bearing capacity and rigidity, they can suffer heavy damage by inelastic plastic deformations or cause huge losses by completely collapsing. A holistic system strengthening technique is required for poor seismic-performance structural systems to increase bearing capacity and rigidity, the limit story drifts ratios, and allow strengthening of the entire structural system to solve structural problems. Furthermore, negative effects on the displacement ductility ratio and energy dissipation capacity should be avoided while increasing RC frames' bearing capacity and rigidity. It is not possible to demolish and renovate all structures with reinforced concrete frame type bearing systems with insufficient earthquake performance level due to the required materials, labor, time required and high cost. It has become an important need to strengthen such structures with an economical method that can be implemented quickly, easily and with little labor, without disturbing the people living inside the structures for a long time. In this way, in the holistic strengthening of the bearing system consisting of RC frames, when the literature is examined, it is seen that the most used technique is the conversion of RC frames into shear walls as a result of removing the brick infill walls in RC frames and replacing them with an RC infill wall (Anil and Altın 2007; Altın et al. 2008b). Although this technique is widely used and preferred, the application difficulties sometimes make it useless. Studies have shown that adding infill walls to RC frames significantly increases the bearing capacity and rigidity of the structural system and limits the story displacements but does not cause reductions in the displacement ductility ratios or energy dissipation capacity values. These factors indicate that this technique is an effective holistic structural system strengthening approach. The disadvantages of this technique are that it takes a long time to apply, the workmanship is difficult, and it prevents the structure from being used for an extended period. This technique is expensive because the structural system has not been used for a long time, and its application is difficult and takes a long time. For this reason, the use of the technique has decreased over time.

In the holistic strengthening of RC frame-bearing systems with insufficient earthquake performance, research has increased on strengthening techniques that can be applied quickly and with less labor before the masonry infill walls in the frame are demolished. For this purpose, strengthening details have been developed using composite materials such as a fiber-reinforced polymer (FRP) bonded to the infill wall surface with epoxy (Altın et al. 2008a, c, 2012). Because of its ease of application and low labor requirements, the strengthening technique of attaching such composite materials to the masonry infill wall surface reduced application time. It caused less discomfort to the building's occupants. However, the main problem with this type of strengthening technique is the high cost of the technique due to the high cost of composite materials and adhesives (Makou 2021). TRM is a composite building material formed by cement-based inorganic mortar and textiles obtained from different materials (such as steel, carbon, basalt, and glass). Textiles used

as strengthening composite material are typically formed from strands of fibers perpendicular to each other (bidirectional). It is understood that TRM has some advantages over Fiber Reinforced Polymers (FRP), considering the production and application of mortar in conventional methods. These advantages are; (a) low cost, (b) resistance to high temperatures, (c) applicable on the concrete, reinforced concrete, and masonry building surfaces, (d) applicable to wet surfaces, (e) low heat permeability, and (f) high bearing capacity. Considering these advantages, researchers have increased the use of TRM in developing strengthening/retrofitting details in the last ten years. Strengthening with TRM was also applied to reinforced concrete frame with masonry infill wall, and positive results were obtained (Koutas et al. 2014).

When the literature was examined, studies were found where mortars containing special additives and fiber types were used for strengthening masonry walls, especially in historical buildings (Mercuri et al. 2023; Vailati et al. 2021; Angiolilli et al. 2020). In addition, studies on increasing the amount of energy dissipation in masonry infill walls and improving the general earthquake performance as a result of special bed-joint sliding placed between the masonry units in masonry infill walls or special layers produced from different materials such as plastic are among the important research topics examined in recent years (Vailati et al. 2023a, b; Mojsilović 2022; Zhang et al. 2022). The development of a cost-effective strengthening technique that can be applied in less time and with less labor, with less inconvenience to the inhabitants of structures with RC frame-bearing systems with insufficient seismic performance levels, continues. There is research in the literature about an innovative strengthening method with a reinforced plaster layer added on the infill wall by connecting the beams and columns, which are the bearing elements of the frame, with anchors, without demolishing the masonry wall inside the frame for the strengthening of RC frames with masonry infill walls with insufficient seismic performance level (Altun et al. 2010; Kaya et al. 2018). The method of strengthening masonry-infilled RC frames by adding a rebar-reinforced stucco layer provides several advantages or benefits compared to adding RC infill walls to RC frames because the application time is shorter, disturbs residents less, and requires less labor. Furthermore, this method is significantly less expensive than adding RC infill walls to RC frames. For these reasons, adding a rebar-reinforced stucco layer to the infill walls is widely used method due to its several benefits for the holistic strengthening of RC frame systems with masonry infill walls with insufficient seismic performance, and the research on this subject has increased (Altun et al. 2010; Kaya et al. 2018). Research has shown that the masonry-infilled RC frames strengthened by adding rebar-reinforced stucco layer strengthening method improve the earthquake performance level of the RC frame bearing system, increase the ultimate load capacity and rigidity, and limit the story drift ratios and damages that occur (Altun et al. 2010; Kaya et al. 2018). In this study, the adding rebar-reinforced stucco layer retrofitting method was chosen to strengthen RC frame systems with masonry infill walls that have poor seismic performance because it affects the inhabitants less, can be applied in a short time with less labor, and low-cost. It has been observed that most studies in the literature ignore the effects of openings that should be in infill walls due to architectural requirements.

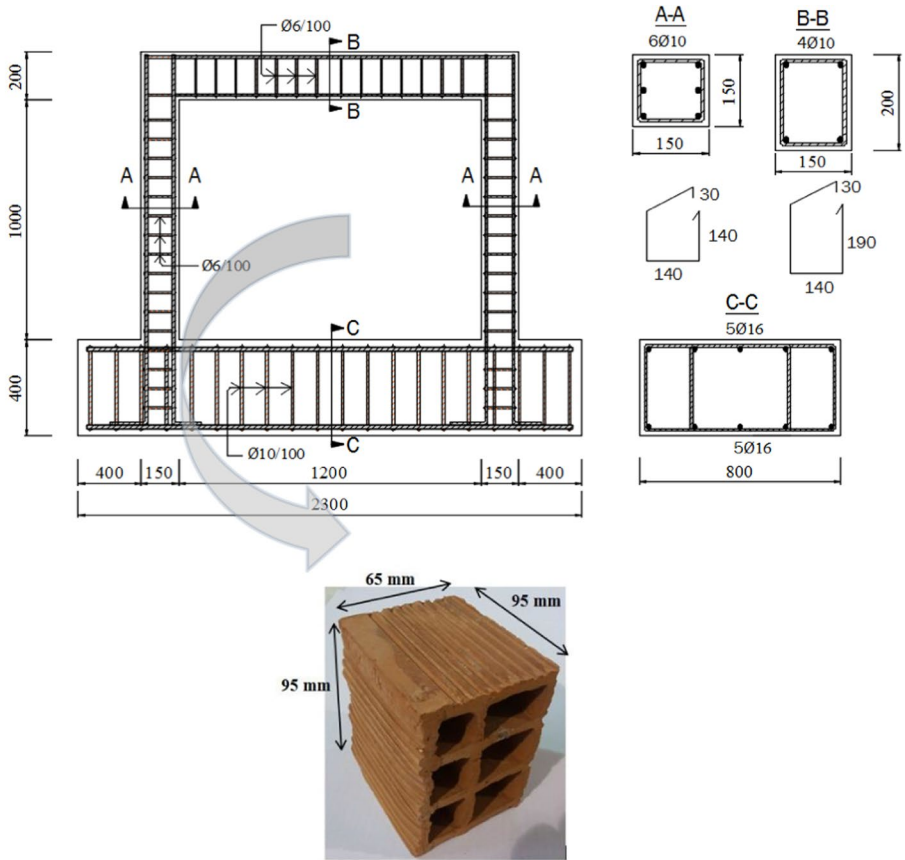
It has been observed that the studies carried out in all of the strengthening techniques applied in RC frame systems with masonry infill walls that have insufficient seismic performance levels and need to be strengthened are generally focused on masonry infill walls that fill the inside of the frame. Most studies generally ignore the effects of openings in the infill wall. The number of research investigating the effects of infill wall opening size and location on earthquake performance and the general behavior of RC frame-bearing systems with masonry infill walls is limited (Ahani et al. 2019; Sigmund and Penava 2013;

Khoshnoud and Marsono 2016; Kakaletsis and Karayannis 2008; Akhoundi et al. 2016; Flippou et al. 2023; Milijaš et al. 2023; Wang 2023; Sakr et al. 2021). Moreover, no study was found in the thorough literature review that investigated the effects of the size and placement of the openings on the strengthening approach used by adding a rebar-reinforced stucco layer to the masonry-infilled RC frames studied within the scope of this study. For this reason, an experimental study was performed, and 11 (1:2 scale) RC frame specimens were produced and tested under the effect of reversing and repeated loading, simulating an earthquake. This study investigated the effects of the changing position and dimension of the openings on the infill wall using the load–displacement behaviors, ultimate load capacities, stiffness, displacement ductility ratios, and energy dissipation capacity values of the specimens. The experimental results obtained from the study are expected to contribute to the literature by containing important findings about how the opening on the infill wall changes the earthquake performance due to architectural requirements. In the second part of the study, nonlinear analysis models of the experiments were created with the ABAQUS finite element software, and the results obtained were compared with the experimental results. The numerical analysis was used to determine whether the ultimate load capacities and general load–displacement behaviors of RC frames with masonry infill walls with openings that were strengthened using the study’s proposed strengthening method could be obtained following the experimental results. In the strengthening technique developed within the scope of this study, the main aim and novelty aspect can be applied in a short time, without disturbing the inhabitants of the building, with less labor without being too complicated, and being a more economical strengthening method by using standard materials without using expensive composite materials. In addition, it is another novelty of the study to investigate how effective the developed strengthening method is in the case of openings such as a door or window spaces left in RC frames with masonry infill walls due to architectural necessities. When the literature is examined, it is seen that the strengthening techniques developed for strengthening RC frames with masonry infill walls are generally developed for situations with infill walls without openings. It is thought that investigating the performance of the strengthening technique developed within the scope of the study on RC frames with masonry infill walls with openings increases the study’s novelty.

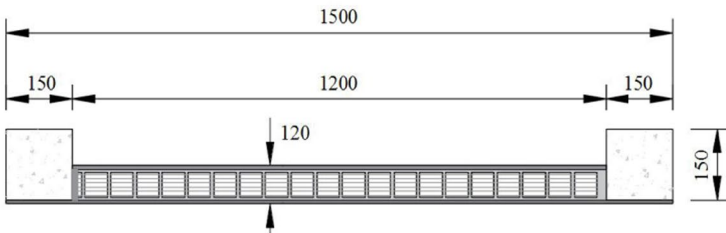
2 Experimental study

2.1 Geometry of the test specimens

Within the scope of the experimental study, it was decided to construct the RC frame specimens with a scale ratio of 1:2. The reinforcement details and geometric dimensions of the RC bare frame specimen are shown in Fig. 1. In addition, these dimensions and reinforcement details are the same for the other 11 specimens. When the dimensions and reinforcement details of the bare frame are examined, it is seen that there are design errors, such as strong beam-weak columns and low shear reinforcement ratios found in structures with poor seismic performance levels in real RC structure insufficient earthquake performance (European Committee for Standardization 2004). The RC bare frame designed within the scope of the study has been produced in a way that includes the design errors that should not be in the RC frame type bearing systems in the Eurocode 8 regulation (European Committee for Standardization 2004) and many similar contemporary earthquake regulations. This approach’s heart is creating a structural system that needs strengthening. Inside the



a) Concrete frame and masonry unit with a scale of 1 to 2



b) Details of masonry unit of infill wall and reinforced beam and column with a scale of 1 to 2

Fig. 1 Dimensions and reinforcement details of the specimens (dimension in mm). **a** Concrete frame and masonry unit with a scale of 1 to 2. **b** Details of masonry unit of infill wall and reinforced beam and column with a scale of 1 to 2

bare frame of the specimens designed for poor seismic performance levels, infill walls were built with masonry similar to the hollow clay brick dimensions of 65×95×95 mm (1:2 scale). Field investigation studies conducted on reinforced concrete structures that

were heavily damaged or completely collapsed after major earthquakes in the world have revealed the important design errors that caused such reinforced concrete structures to receive heavy damage or collapse. The main design errors that cause reinforced concrete structures to be severely damaged or completely collapse due to earthquake effects are plastic hinges in the columns in the load-bearing systems designed as strong beams and weak columns in reinforced concrete frames and undesirable collapse of the structural system by exhibiting a column collapse mechanism. Another prominent design deficiency was the occurrence of shear failure, which is an undesirable sudden and brittle collapse mechanism in the load-bearing elements due to inadequate placement of shear reinforcement in columns and beams in the structural load-bearing system. Another design error encountered is the formation of plastic hinges at the connection node or on the column in reinforced concrete frames as a result of not tightening the shear reinforcement spacing at the column-beam connection nodes. It is aimed to examine how successful the strengthening technique developed within the scope of the study can be in structures that actually have all of these design errors by applying it on a reinforced concrete frame with extremely inadequate earthquake performance, where all three of these design errors are present.

The characteristics of the experimental specimens in the experimental program are presented in Table 1 by associating them with the experimental variables. In the experimental program, 11 specimens were produced, including one RC bare frame without infill walls, 5 test specimens with masonry infill walls without strengthening, and five specimens with masonry infill walls strengthened by adding reinforced stucco layers. Specimen-2 and Specimen-7 are masonry infill walls without openings, without strengthened and strengthened specimens, respectively. Specimen-3 and Specimen-4 are masonry infill walls with openings of 400×480 mm and 500×600 mm, respectively, in the center of the wall. In Specimen-5 and Specimen-6, the same size opening was located close to the column joint and beam in the upper left corner of the masonry infill wall. The positions and dimensions of the openings left in the specimens are given in Fig. 2.

2.2 Materials

Specimens-8, 9, 10, and 11 were made the same way as Specimens-3, 4, 5, and 6, masonry infilled wall specimens with openings but was strengthened by adding a rebar-reinforced stucco layer. The corresponding openings of the Q131/131 (made by fabrication welding of deformed reinforcement bars with a diameter of 5 mm in both directions and 150 mm intervals) class mesh steel reinforcement placed in the stucco layer were cut out in the strengthened specimens. Furthermore, there are no other special reinforcement details in the stucco layer around or at the corners of the openings. While producing the specimens, 25 MPa concrete compressive strength was determined as the target strength. While pouring the RC bare frame of each test specimen, five 150×150 mm standard cube samples were taken and stored under the same curing conditions as the specimens. Following the concrete pouring of the specimens, five cube samples and test specimens were removed from the mold, cured by wrapping them in wet sacks for seven days, and then allowed to dry in the laboratory for 21 days. Cube concrete samples were stored and cured in the laboratory, in the same environment as the specimens. The day after they were cast, they were removed from the mold, cured with a wet sack and plastic tarpaulin for 7 days, and left to dry under normal room conditions in the laboratory for the remaining 21 days. Five cube samples taken from the specimens were stored until the day of the tests to determine the concrete compressive strength. Compression tests were performed on the five samples on the same day

Table 1 Properties of specimens

Spec. #	Compressive strength of		Opening		Remarks
	Concrete f_c (MPa)	Adding mortar layer f_M (MPa)	Size (mm)	Location	
1	25.0	7.9	–	–	Bare frame without masonry wall
2	24.8	8.0	–	–	Masonry-infilled RC frame without opening and strengthening
3	24.5	7.5	400×480	Center of Infill	Masonry-infilled RC frame with opening and without strengthening
4	25.1	7.7	500×600	Corner of Infill	
5	24.9	7.8	400×480	Corner of Infill	
6	24.7	8.0	500×600	Corner of Infill	
7	25.1	7.5	–	–	Masonry-infilled RC frame without opening and with strengthening
8	24.8	8.1	400×480	Center of Infill	Masonry-infilled RC frame with opening and strengthening
9	25.0	7.9	500×600	Corner of Infill	
10	24.9	8.0	400×480	Corner of Infill	
11	24.6	7.6	500×600	Corner of Infill	

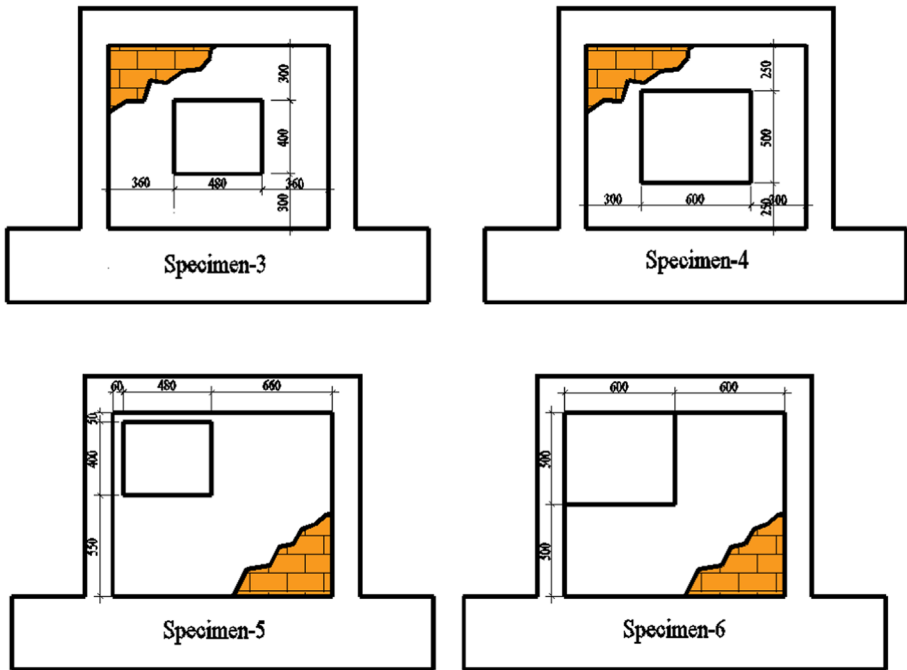


Fig. 2 The Opening Layout of the Specimen (Dimension in mm)

as the experiments, and their compressive strengths were determined. Five cube samples were tested using a computer-controlled hydraulic press with a constant loading speed of 0.5 kN/s. The average of the concrete compressive strength values obtained from five concrete cube samples taken for each bare RC frame specimen is given in Table 1. Since these values obtained from five cube samples are very close to each other, the standard deviation and variance values are extremely small. The average concrete compressive strength values given for the specimens in Table 1 ranged between 25.10 MPa and 24.50 MPa, with the standard deviation and variance values calculated as 0.19 MPa and 0.04 MPa, respectively. These values are very close to the targeted 25 MPa concrete compressive strength.

The masonry infill walls of the specimens were constructed using the mortar mixture. After the infill wall was finished, the wall's interior and exterior surfaces were plastered with the same mortar. Five 50×50 mm cube samples of the mortar mixture used to construct, and plaster masonry infill walls were obtained, and their compressive strength was examined. Cube samples taken from the mortar used in masonry infill walls were cured like samples taken from the RC bare frame. It was stored under the same conditions until the day of the experiments, and then the compressive strength values were determined by performing the test. The averages of the compressive strength values obtained from five cube mortars for each specimen, taken from the masonry infill walls of the specimens, are given in Table 1. The specimens' average mortar compressive strength values range between 8.10 and 7.50 MPa, near the desired 8 MPa value. Additionally, the standard deviation and variance values of the average mortar strength values measured for the specimens were computed to be 0.20 MPa and 0.04 MPa, which are very low values. The rebars used to make the specimens were purchased simultaneously, and their mechanical characteristics were guaranteed to be identical. The mechanical strength values were measured using

the axial tensile test on five samples of each rebar type utilized in the specimens. Average mechanical strength values obtained from five samples tested for each reinforcement type are given in Table 2. Under computer control, the reinforcement samples were subjected to an axial tensile test with a constant loading speed (0.1 mm/s).

2.3 Strengthening procedure of specimens

This strengthening method places Q131/131 class reinforcing mesh in the stucco layer. A standard mesh reinforcement will be placed inside the reinforced stucco layer to make the application easier. The mesh reinforcement sample's strength values were determined similarly to other RC bare frame reinforcement types, as shown in Table 2. Following the production of the RC bare frames, the brick infill walls of the specimens were built, the inner and outer surfaces were covered with stucco, and the test elements were made ready for strengthening application.

In Fig. 1b, the existing plaster layer on the masonry infill wall is shown in the section of the RC frame with masonry infill walls without strengthening. It is clearly seen that the thickness of the masonry unit is 95 mm and after the application of plaster on both sides, the thickness of the infill wall is 120 mm. With the addition of a 30 mm thick reinforced stucco layer placed on the inner face of the infill wall frames for strengthening, the total infill wall thickness reaches 150 mm, the same thickness as the column. It can be seen from the B-B sections given in Fig. 3 that the column and infill wall reached the same thickness after strengthening. The masonry infill wall thickness increased to 120 mm when the test specimens' masonry infill walls were coated with 12.5 mm of plaster from the inner and exterior surfaces. After this stage, 28 days waited for the mortar and surface plaster used in the masonry infill wall to gain strength. Anchor holes were drilled in the RC frame and masonry infill walls so that the RC frame and masonry infill walls could perform together with the additional rebar-reinforced stucco layer. "L"-shaped anchor reinforcements ensure the stucco layer reinforcements and the infill wall work together. Anchor holes are drilled on the infill wall for these reinforcements. The holes drilled for the straight anchors in the RC bare frame and the "L" shaped anchors used in the infill wall are 8 mm, while the anchors' diameters are 6 mm. For both types of anchoring, plain rebars with a 6 mm diameter were used. Figure 3 shows the strengthening details, anchor arrangement, and the number of anchors for the strengthened specimens Specimen-7, 8, 9, 10, and 11. After the drilling, the anchor holes were cleaned of dust and loose particles with compressed air. Following this, a double-sided, five mm-diameter Q131/131 reinforcing mesh cage with 150 mm spacing was placed within the stucco layer to be added to the masonry infill wall surface. The mesh reinforcements are fixed with wires to the reinforcements anchored to the RC bare frame and to the "L"-shaped anchors placed in the holes drilled on the

Table 2 Mechanical properties of reinforcement

Diameter (mm)	Type	Yield strength (MPa)	Failure strength (MPa)	Modulus of elasticity (GPa)
5	Ribbed	576	615	207
6	Plain	330	410	202
10	Ribbed	544	585	205
16	Ribbed	539	575	206

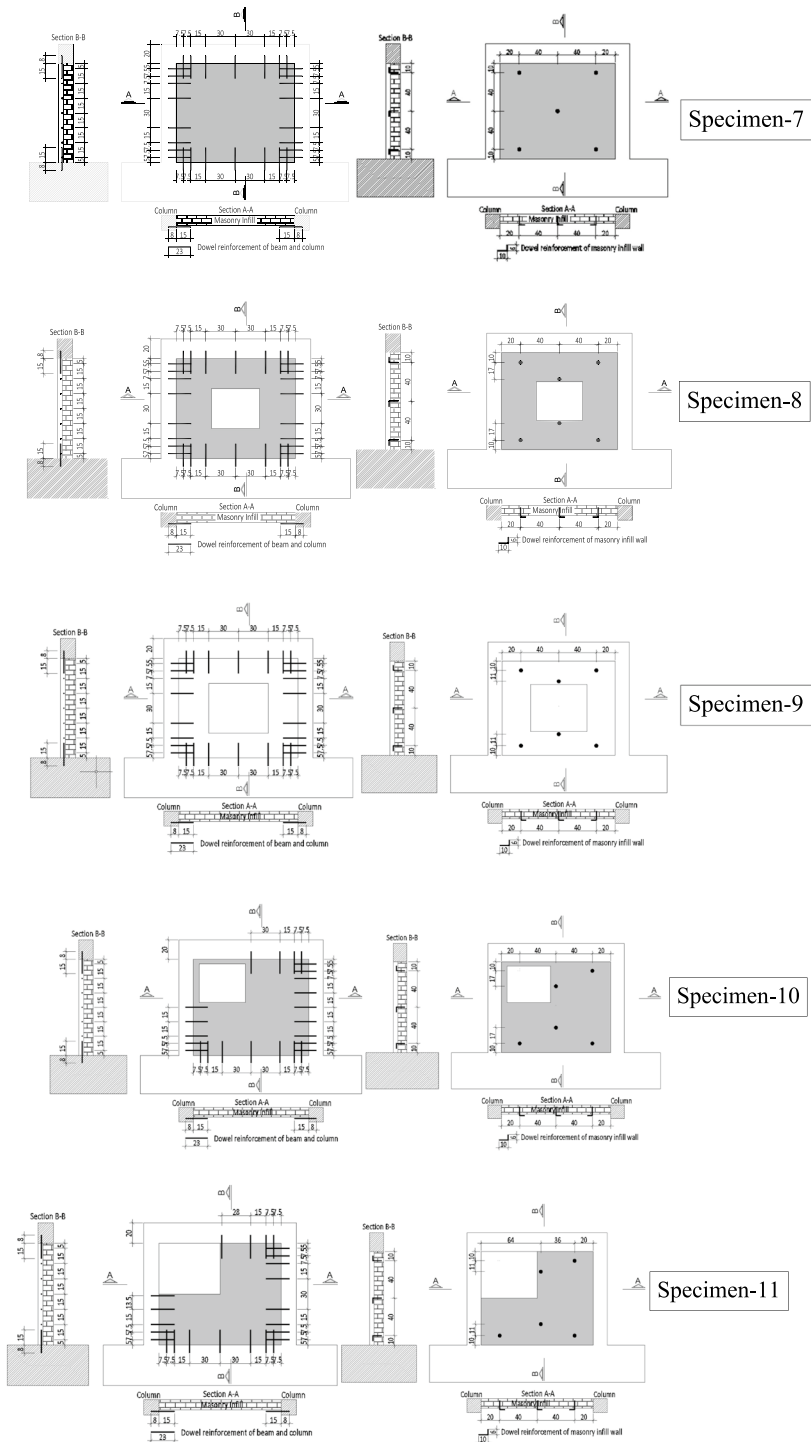


Fig. 3 Strengthening details of the specimens (Dimension in mm)

masonry infill wall surface. Sikadur 31, an anchoring epoxy from Sika Company, was used to attach the anchors to the holes drilled in the RC bare frame and masonry infill wall surface. The properties of Sikadur 31 epoxy used for anchors are given in Table 3, and these values are the minimum mechanical strength values provided by the manufacturer. After placing the mesh reinforcements and anchors on the stucco layer was added to strengthen the infill wall, it waited 48 h for the epoxy to gain its strength. The strengthening procedure was then completed by applying a 30 mm-thick stucco layer to the mesh reinforcement, which was used for laying and plastering the masonry infill wall, with a target compressive strength of 8.0 MPa, produced using the same mortar material mixture. After 28 days were completed by applying curing processes on this layer and the stucco layer had reached its strength, the strengthened specimens became ready to be tested. The examples selected from photographs showing the strengthening process steps applied to the specimens are presented in Fig. 4. RC frames of the specimens were produced, and then the masonry infill walls were built according to the experimental variables and made ready for plastering. Both sides of the masonry infill walls were plastered, and the specimens were made ready for strengthening. In the strengthening technique developed after this stage, the holes of the anchors to be used to connect the RC frame, masonry infill wall, and the stucco layer to be added were prepared by drilling the details as given in Fig. 3. The anchors used in the RC frame are flat, and the anchors used on the infill wall surface are "L" shaped. After this stage, the anchor holes opened were cleaned with compressed air and made ready for epoxy injection. Sikadur 31 epoxy was injected into the cleaned anchor holes, and the Q131/131 reinforcing mesh cage, which would remain in the stucco layer, was embedded before the anchors were placed. Then, anchors were inserted into the epoxy-injected holes, and the anchors were fixed by connecting them to the reinforcement cage with wires. After waiting 48 h for the epoxy to complete its curing and reach its full strength, a 30 mm thick stucco layer was placed on the reinforcement by applying it as it was. The plastered specimens were ready to be tested after 28 days of curing and waiting to reach the stucco layer strength.

The strengthening technique intended to be developed within the scope of this study is aimed to be used in RC frames with masonry infill walls in standard residential type RC structures with inadequate earthquake performance. For this reason, efforts have been made to ensure that the strengthening technique developed is an economical strengthening method that disturbs the people living inside the buildings as little as possible, can be applied in a short time, can be applied from inside the building without installing any scaffolding outside the building, can be done with little labor, and is economical. The strengthening method developed by taking this approach and design philosophy into consideration has been designed as a method that can be applied only to the inner surface of masonry infill walls, from within the structure. In this way, there will be no need to

Table 3 Properties of Sikadur 31 Epoxy

Remarks	Value*
Compression strength	60–70 N/mm ²
Flexural tension strength	30–40 N/mm ²
Axial tension strength	15–20 N/mm ²
Bonding strength	> 4 N/mm ²
Elastic modulus	4300 N/mm ²

*The manufacturer provides these values



Fig. 4 Strengthening application step photos of specimens

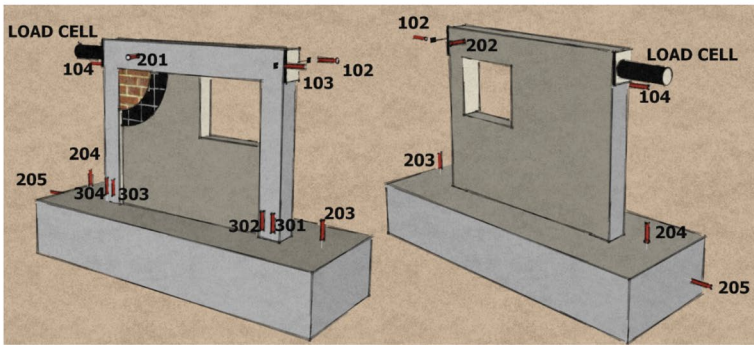
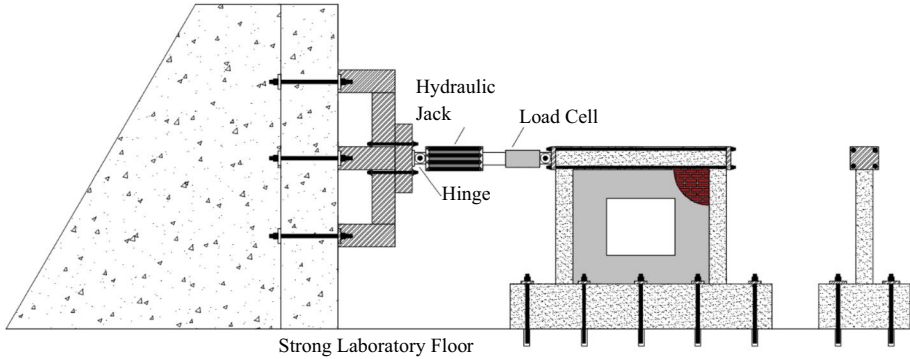
install a scaffolding outside the building and the application time will be shortened. Shortening the application time and reducing labor will make the strengthening technique more economical.

2.4 Test setup and instrumentations

The tests of the specimens were carried out with the support of the laboratory's rigid wall and floor system and using the loading system installed on the rigid wall. Experiments were conducted in Süleyman Demirel University Civil Engineering Department Structural Mechanics Laboratory. Horizontal reversible repeated loading, simulating the earthquake to the specimens, was applied to the RC frame beam from floor level by a hydraulic loading system with a capacity of 1000 kN and measured with a load cell of 600 kN. Story displacement, rigid mass movements, and measurements collected by a data logger system using Linear Variable Differential Transformers (LVDT) on the specimens were transferred to the computer and used in the evaluations. The details of the test and measurement system during the tests of the specimens are presented in Fig. 5. The tests of the RC frame specimens with masonry infill walls were followed and carried out by drawing load-story displacement graphs. The applied loading history of specimens was identified and shown in Fig. 6 using ACI 374.1-0 2005 regulation (American Concrete Institute 2005). The tests were carried out in displacement control, according to the change of story drift ratio. The 12 different reversed story drift ratio was applied to the specimens. Full cycles are three for each interstorey drift threshold, for a total cycles of 3×12 . Applied story drift ratios of specimens are shown in Fig. 6. The drift ratio was calculated as the ratio of corrected story displacement to the RC frame's total height. The story displacement of the specimens was measured from the midpoint of the RC frame beam. Errors in story displacement due to rigid sliding and rotational deformations that may occur in the specimens have been corrected. The corrected story displacement value was calculated by calculating the displacement values that rigid sliding and rotational deformations could cause in the story displacement and subtracting them from the measured value, and load–displacement graphs were drawn using this value. The loading history, details of which are given in Fig. 6, was tried to be applied to all specimens in an identical manner. However, after the ultimate load capacity value was reached in the specimens, each specimen started to lose its ultimate load at different story drift ratios. The cycles after the story drift ratio decreased by 15% in the ultimate load capacity values of the specimens were not applied and the test was terminated.

3 Experimental results and discussions

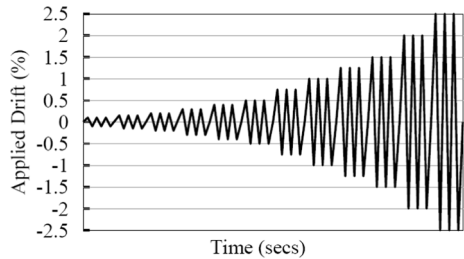
As a result of the tests on the specimens, the load–displacement behavior of the RC frame systems with opening masonry infill walls was obtained. The specimens' ultimate load capacity, initial stiffness, displacement ductility ratios, and energy dissipation capacity values were calculated using these graphs. The load–displacement graphs obtained as a result of the tests on the specimens are presented in Fig. 7. The envelope graphs of the specimens were drawn by combining the peaks of the loading cycles applied in line with the loading history, the details of which are given in Fig. 6 and comparatively presented in Fig. 8. The ultimate load capacity values of the specimens were determined using the maximum load values reached for both forward and



Sensors number	Remarks
101	Load Cell
102, 103, 104	Lateral Story Displacement of RC Frame
201, 202	Out of Plane Displacement of RC Frame
203, 204	Rigid Body Turning Displacement of RC Frame Foundation
205	Rigid Body Sliding Displacement of RC Frame Foundation
301, 302, 303, 304	RC Frame Columns Moment-Curvature Measurements

Fig. 5 Test setup and instrumentations

Fig. 6 Applied loading history of the specimens



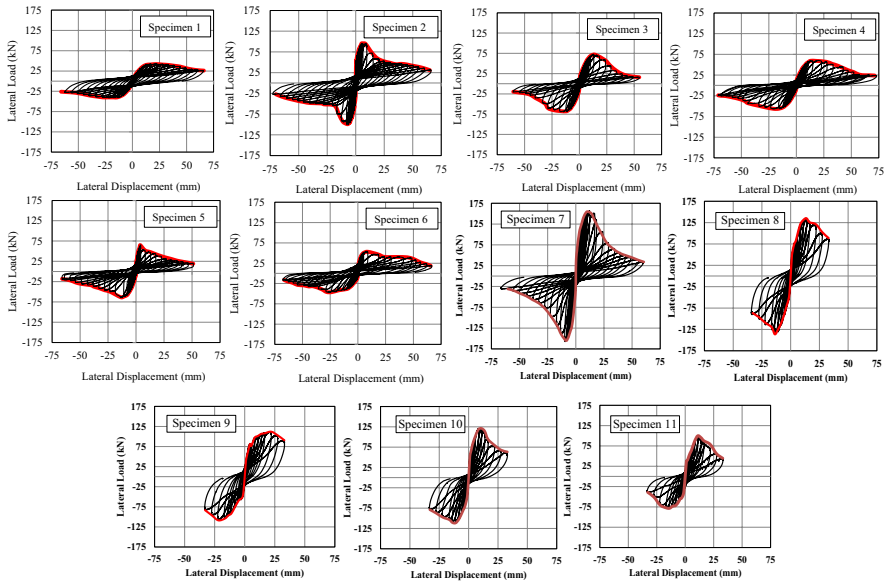
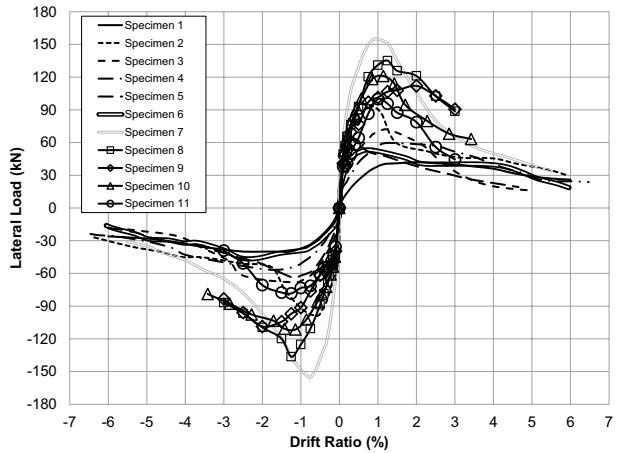


Fig. 7 Lateral load-displacements graphs of specimens

Fig. 8 Load–displacement envelope strength graphs of specimens



backward loading cycles using the envelope graphs given in Fig. 8. In addition, the story drift ratios of the specimens were calculated by dividing the displacement values at which the ultimate load capacity was achieved in the forward and backward cycles by the frame story height. The story drift ratio values were calculated for the forward and backward cycles.

The initial stiffness values for the forward and backward cycles were calculated using the slope of the lines connecting the first forward and backward loading cycle peaks applied to the specimens to the origin. An initial stiffness value was obtained for each specimen by taking the average of these two values. Envelope graphs were used to calculate the displacement ductility ratios of the specimens. The point where the ultimate

load capacity of the specimens decreased by 15% was accepted as the failure point (Anil and Altın 2007; Altın et al. 2008a, b, c, 2012, 2010; Makou 2021; Koutas et al. 2014; Mercuri et al. 2023; Vailati et al. 2021, 2023a, b; Angiolilli et al. 2020; Mojsilović 2022; Zhang et al. 2022; Kaya et al. 2018). The other displacement value used in calculating the displacement ductility ratio was determined as the displacement of the peak point of the first loading cycle where the horizontal movement started in the load–displacement graph of the specimens. The displacement ductility ratio values were calculated by proportioning the failure point displacement value to the displacement value of the point where the horizontal movement started in the load–displacement graph of the specimens. These calculations were made separately for both forward and backward cycles. A displacement ductility ratio value was obtained for each specimen by taking the average of both displacement ductility ratio values. The energy dissipation capacity values of the specimens were calculated by calculating the area under the sections of the load–displacement graphs up to the failure point by adding them cumulatively. The area under each loading cycle in the sections up to the failure point of the load–displacement graphs was calculated separately. The specimens' cumulative energy dissipation capacity values were obtained by summing the calculated area for each cycle. The results of the specimens were calculated and presented in Table 4 (Anil and Altın 2007; Altın et al. 2008a, b, c, 2012, 2010; Kaya et al. 2018).

The proposed strengthening method within the study's scope improves RC frames' general load–displacement behavior with opening masonry infill walls and improves their performance under earthquake loading. The applied strengthening method increased the ultimate load capacity, initial stiffness, and energy dissipation capacity values of reinforced concrete frames with masonry infill walls by 83%, 226%, and 62%, respectively, but resulted in a 38% decrease in displacement-ductility ratios. The values given were calculated by taking the average of the values obtained for all test elements. In the developed strengthening method, the reinforced stucco layer placed in front of the masonry infill wall is connected with both the infill wall and the RC frame with anchors. It is thought that this technique applied after the horizontal earthquake loading acting on the RC frame is transmitted to the masonry infill wall together with the reinforced stucco layer. A larger part of

Table 4 Experimental Results

Spec #	Ultimate load capacity (kN)		Drift ratio at ultimate load (%)		Initial stiffness (kN/mm)	Displacement ductility ratio	Cumulative energy dissipation capacity (kN-mm)
	Forward	Backward	Forward	Backward			
1	42.00	−40.00	2.00	1.27	7.64	3.33	2416
2	95.00	−98.77	0.46	0.72	57.08	2.54	6286
3	72.15	−68.03	1.18	1.10	28.66	2.15	5831
4	59.43	−56.43	1.18	1.89	21.42	2.04	4148
5	64.92	−63.61	0.35	1.23	24.36	1.90	5146
6	53.20	−46.16	0.80	2.14	19.88	1.73	4005
7	157.30	−157.59	0.93	0.80	562.50	1.50	11,282
8	135.12	−136.41	1.25	1.25	41.82	1.40	8968
9	112.01	−108.67	2.00	2.00	36.56	1.38	7176
10	121.05	−111.44	1.14	1.14	38.76	1.75	7178
11	99.88	−78.37	1.00	1.25	33.48	1.55	6521

the infill wall works effectively. It contributes to the bearing capacity, stiffness, and energy dissipation capacity. As it is known, masonry infill walls that are not strengthened can be transferred effectively only in very small parts of the diagonal direction under reversible and repeated horizontal earthquake loading. In these small areas at the corners of the infill walls, where the horizontal earthquake load is transferred from the RC frames, the masonry reaches collapse in the RC frames with infill walls due to the crushing of the bricks or the separations in the infill wall joints in the diagonal lines. The stucco layer added in front of the infill wall with the strengthening method developed within the scope of this study, connecting both the infill wall and the RC frame with anchors, delayed the separation of the infill wall from the RC frame and played an active role in the bearing of the horizontal earthquake loading in a much larger part of the infill wall. In addition, the reinforced stucco layer added to the front part of the infill wall increased not only the bearing capacity and stiffness but also the energy dissipation capacity, thereby improving the behavior of masonry infill walls, which exhibit an extremely brittle fracture mechanism under the effect of earthquake loading.

The ultimate load capacity, initial stiffness, and energy dissipation capacity values of the strengthened Specimen-7 without opening masonry infill wall exhibited higher values by 66%, 885%, and 79%, respectively, than the Specimen-2 without strengthening. The displacement ductility ratio of Specimen-7 is 69% smaller than Specimen-2. The strengthening technique used on the masonry-infilled RC frame with opening specimens increased the ultimate load capacity, initial stiffness, and energy dissipation capacity values by 87%, 61%, and 57%, respectively, while decreasing the displacement ductility ratio by 30%. The strengthening technique proposed within the study's scope was successful when evaluated in terms of ultimate load capacity and energy dissipation capacity. All specimens with openings that were strengthened by adding a reinforced stucco layer passed Specimen-2 without strengthening in terms of ultimate load capacity and energy dissipation capacity. The ultimate load capacity values and energy dissipation capacities of the strengthened specimens with openings were calculated to be 23% and 19% higher on average than the Specimen-2 without strengthening, respectively. However, the applied strengthening technique was unsuccessful in raising the initial stiffness and displacement ductility ratios of the masonry-infilled RC frame specimens to the level of Specimen-2 without strengthening. Specimen-2 without opening and strengthening has 53% higher initial stiffness and 69% higher displacement ductility ratio values than the strengthened specimens with openings. Of course, the main reason for the low success in stiffness and displacement ductility ratio is the openings in the masonry infill walls. However, the applied strengthening method demonstrated a significantly successful performance and managed to increase the ultimate load capacity and energy dissipation capacity values of the specimen's masonry infill walls with openings to the level of the Specimen-2 with infill walls without opening and even above. With the strengthening applied, the negative impact of the openings in the ultimate load capacity and energy dissipation capacity performance indicators was completely eliminated and an even higher performance was achieved.

3.1 Effects of opening size on experimental results

The effects of the masonry infill walls' opening sizes on the RC frame systems are one of the factors investigated. When the results of the specimens without strengthened are examined, it is clear that the general load–displacement behavior of RC frame systems with masonry infill walls is negatively affected, and their performance under earthquake loading

decreases as the size of the opening on the masonry infill wall increases. The increase in the ratio of the opening area to the masonry infill wall area from 16 to 25% in the specimens with masonry infill walls without strengthening with opening affected the earthquake performance negatively. The ultimate load capacity, initial stiffness, displacement ductility ratios, and energy dissipation capacity values all decreased by an average of 22%, 28%, 8%, and 35%, respectively, in the specimens with masonry infill walls without strengthening with the opening. The increase in the size of the openings resulted in a decrease in all of the significant seismic performance parameters. A similar trend was seen in the strengthened specimens. Despite the effect of the strengthening method and an increase in the ultimate load capacity, initial stiffness, displacement ductility ratio, and energy dissipation capacities of the strengthened RC frames with masonry infill walls with openings, the expansion of the opening in the masonry infill walls harmed the seismic performance of the strengthened specimens. The increase in the opening area ratio to the total frame area from 16 to 25% in the strengthened masonry infill wall specimens with an opening and strengthening also negatively affected the seismic performance, similar to those without strengthening. The ultimate load capacity, initial stiffness, displacement ductility ratio, and energy dissipation capacity values of the strengthened masonry infill wall specimens with opening were decreased by an average of 21%, 15%, 13%, and 18%, respectively. The size of the openings left in the masonry infill walls has been extremely effective on the general behavior of the RC frames with infill walls under earthquake loading, bearing capacity, stiffness, and energy dissipation capacities, and caused a significant decrease in all of them. It is known that the behavior of RC frames with infill walls under the effect of horizontal earthquake loading is calculated with an approach known as the strut-tie method, which calculates the contribution of infill walls to the horizontal load-bearing capacity. The increase in the size of the opening left in the infill walls prevents the formation of diagonal bars in the infill wall from transferring the horizontal load and highly limits the contribution of the infill walls to the bearing strength, stiffness, and energy dissipation capacity. The strengthening of the masonry infill walls with the reinforced stucco layer developed within the scope of this study and the attachment of the added reinforced stucco layer to the RC frame and the infill wall with anchors provided a much more efficient and uniform distribution of the horizontal earthquake loading acting on the RC frame to the masonry infill wall and the reinforced stucco layer. The negative effects of the infill wall of the opening on the load bearing and transmission mechanism have been reduced by the applied strengthening technique, and the infill wall has been provided to contribute to the bearing capacity more effectively.

3.2 Effects of opening location on experimental results

Another variable examined in the study was the change in the positions of the openings left in the masonry infill walls. Openings in the middle or near the corner of the masonry infill wall affected the load–displacement behavior and earthquake performance. Depending on whether the opening is at the corner or middle of the masonry infill wall, the load–displacement behavior and earthquake performance have been negatively affected. The ultimate load capacity, initial stiffness, displacement ductility ratio, and energy dissipation capacity values of the specimens decrease by an average of 11%, 13%, 16%, and 8%, depending on whether the opening is at the corner or the middle of the masonry infill wall. Similarly, the opening at the corner reduced the ultimate load capacity, initial stiffness, displacement ductility ratios, and energy dissipation capacity values by 12%, 9%, 8%, and 17%, respectively,

compared to the opening in the middle. The variables investigated within the scope of the experimental study and the applied strengthening technique caused significant differences in the failure mechanisms of masonry-infilled RC frames with openings and affected the damage distribution. Figure 9 shows photographs of the damage distributions and failure mechanisms obtained after the completed experiments.

When the collapse mechanisms in Fig. 9 are examined, the bare RC frame (Specimen-1) failure mechanisms and the masonry-infilled RC frame without opening and strengthening (Specimen-2) in the experimental study are as expected. Specimen-1 showed a typical column collapse mechanism after the plastic hinges developed in the top and bottom regions of the RC bare frame columns. Specimen-1, which collapsed by exhibiting an undesirable collapse mechanism, behaved as expected, as observed in real structures with poor seismic performance RC bare frames. The position of the openings left in the infill walls is an important parameter affecting the bearing capacity, stiffness, and energy dissipation capacities of RC frames with infill walls under earthquake loading. If the opening is in the middle or corner of the infill wall, the horizontal earthquake loading transmission mechanism transferred from the RC frame to the infill wall changes. The fact that the opening is located in the middle of the infill wall dividing the infill wall into two wing walls and being in the form of a wing wall to support the RC frame columns causes a more effective load transfer mechanism to be formed than if the opening is positioned at the edge and in the form of a single infill wall section. The infill wall being in the form of two wing pieces has caused each infill wall to create its own diagonal strut and tie mechanism, to transfer the earthquake load and contribute more effectively to the bearing capacity, stiffness, and energy dissipation capacity. In addition, the fact that the infill walls are adjacent to the frame columns on both sides has also prevented the formation of a short column collapse mechanism in the columns. Positioning the opening at the edge caused the frame column on the side without the infill wall to show short column behavior. The infill wall part under the opening could not contribute effectively to the bearing capacity, stiffness, and energy

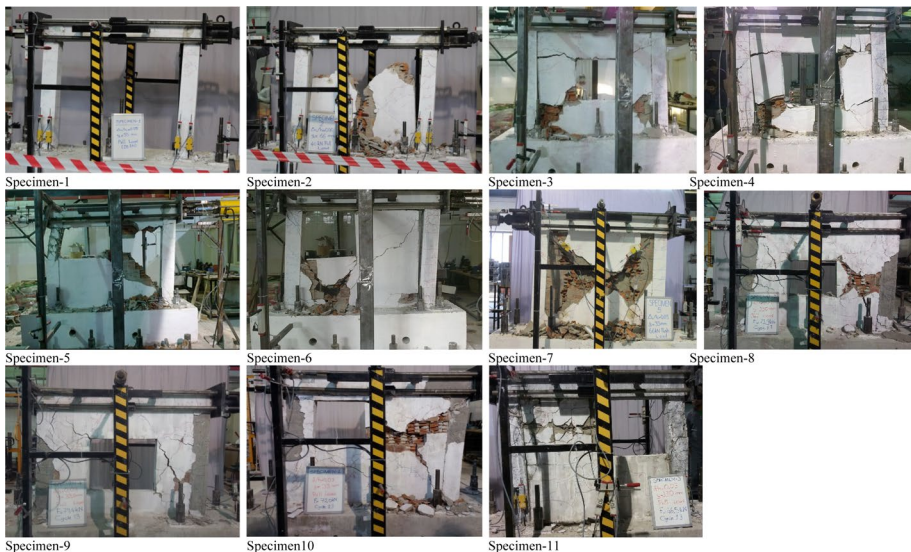


Fig. 9 Failure modes of specimens after the test

dissipation capacity. The strengthening method developed within the scope of this study connects the infill wall and the RC frame in a much better way through the added reinforced stucco layer. With the anchors added into the reinforced stucco layer, the masonry infill wall, and the anchors added to the RC frame, the reinforced stucco layer was connected to each other, creating a more effective load transfer mechanism. Although the positions of the openings left in the infill wall are still effective on the collapse mechanism, the effects of the openings on the failure mechanism became evident later on due to the increased story displacement at much larger story drift ratios. When the opening is placed at the corner of the RC frame, the short column behavior that occurs in the frame column in the failure mechanism has also been observed in the strengthened specimens. However, shear failure of the column occurred at much larger story displacement values until much higher bearing strength, stiffness, and energy dissipation capacity were reached, and the overall performance level increased under the effect of earthquake loading.

3.3 Failure modes of specimens

The masonry infill wall without opening (Specimen-2) specimen also behaved as expected, and the masonry infill wall that filled the inside of the RC frame delayed the collapse of the RC bare frame by exhibiting a column collapse mechanism, thereby increasing the ultimate load capacity, rigidity, and energy dissipation capacity values. The crushing at the upper corners of the masonry infill wall and the "X"-shaped shear cracks in the infill wall removed the infill wall's positive contribution to the load-bearing system, and the RC bare frame collapsed via a column mechanism. In Specimen-2, which has an infill wall without opening and strengthening, the horizontal earthquake loading was transferred from the RC frame to the masonry infill wall with the imaginary diagonal bars formed in the masonry infill wall. However, due to local damages occurring in the upper corners of the RC frame at the ends of the imaginary masonry diagonal bars where the earthquake load is transferred to the masonry infill wall, the positive contributions of the masonry infill wall to the rigidity and horizontal force carrying capacity of the RC frame bearing system remained limited. The masonry infill wall was disabled before it could be used completely and did not effectively contribute to the performance of the bearing system. Similar failure mechanisms were observed in Specimen-3 and Specimen-4, which have a symmetry axis opening in the center of the masonry infill walls. The openings left in the middle of the infill wall divided the masonry infill wall into two wing walls, and these wing infill walls on the left and right of the openings behaved like two independent wall pieces. Diagonal cracks were developed towards the frame corners from the corner areas where stress concentrations of the openings were left in the center of the infill wall. The wing infill walls on the left and right received heavy shear damage in the direction of the opening's lower edge, crushing the infill walls and causing the specimens to collapse. The cross-sectional areas of the wing walls on both sides of the opening are smaller because the opening in Specimen-4 is larger. As a result, shear damage at the opening's lower corners and crushing on the infill wall were more severe. The openings left in the masonry infill walls of the Specimen-3 and Specimen-4 at the middle axis of symmetry caused the infill walls to be divided into two parts as two wing walls and prevented the formation of a pair of crossed bars as in Specimen-2. In Specimen-3 and Specimen-4, separate cross diagonal bars were formed on each of the wing infill walls on both sides of the opening. The damage to the wing infill walls of Specimen-3 and Specimen-4 occurred in the form of crushing on the masonry infill walls at the lower corners of the wing walls on both sides where they meet the RC frame. In the

upper parts of the wing walls on both sides of the openings, the shear cracks starting from the corner of the opening have widened. The failure mechanism in masonry-infilled RC frames has entirely changed in Specimen-5 and Specimen-6, where the openings are positioned at the frame's corners. Short column behavior was observed in the specimens where the opening was close to the corner region, and the column received heavy shear damage in this region. In Specimen-5 and Specimen-6, where the openings left in the infill wall are located at the corner of the frame, a short column collapse mechanism occurred in the RC frame column that is not supported by the wing infill wall and is adjacent to the opening, while crushing was observed in the infill wall section located at the edge of the opening, starting from the corners of the diagonal bars. While the crushing occurring in the area where the bottom corner of the RC frame and the infill wall meet was more effective in Specimen-5, this crushing remained in a more localized, smaller area in Specimen-6. The shear damage in the column of Specimen-5 adjacent to the opening was much greater than that of Specimen-6 and the column was much more severely damaged.

Strengthened Specimen-7 without opening and other strengthened specimens with openings have revealed that diagonal cracks occurring in the entire infill wall are not localized in the direction of the RC frame's main diagonal or at the opening's corners, and shear cracks spread throughout the infill wall. By forming a single main shear crack in the diagonal direction, the stucco layer prevented the masonry infill wall from being crushed in a small area at the corners or collapsing. With the applied strengthening method, the masonry infill wall placed within the RC frame and the beams and columns forming the RC frame were combined with anchors and reinforced stucco layer, ensuring that the horizontal earthquake force applied to the frame was distributed much better to the parts that make up the entire structural system. In the specimens where the strengthening method was not applied, the positive contribution of the infill walls to the bearing capacity, rigidity and general behavior of the system was eliminated as a result of crushing in local small areas that occurred at the corner points in the direction of the diagonal of the RC frame in the masonry infill wall, while in the strengthened specimens, the masonry infill walls continued to contribute to the earthquake performance of the system. In the applied strengthening method, the reinforced stucco layer placed in front of the masonry infill walls distributed the horizontal earthquake load from the RC frame through anchors throughout the masonry infill wall and caused the infill wall to contribute to the bearing capacity, rigidity and general earthquake performance in a much more efficient way. As a result, the horizontal earthquake load transferred from the RC frame to the masonry infill wall is distributed throughout the infill wall. When the failure mechanisms of Specimen-7, 8, 9, 10, and 11 in the strengthened test series were examined, it was observed that the applied strengthening method was extremely effective on the behavior of the specimens and significantly changed the failure mechanisms.

In addition to the positive effects of the strengthening method developed within the scope of the study on the earthquake performance, general load displacement behavior, ultimate load capacity, stiffness, displacement ductility ratios and energy dissipation capacities of RC frames with masonry infill walls with openings, it also affects the damage and crack distribution by changing the collapse mechanisms. In order to see that it has a positive effect, the crack distributions of the strengthened specimens with openings are given in Fig. 10. When the crack distributions given in Fig. 10 are examined, it is shown that the strengthening technique developed within the scope of the study prevents cracks and damage from concentrating in a local region in the end regions of the bars in the direction of the diagonals of the masonry infill walls. The strengthening method has shown that the cracks are distributed over the entire infill wall surface and the masonry infill wall contributes to

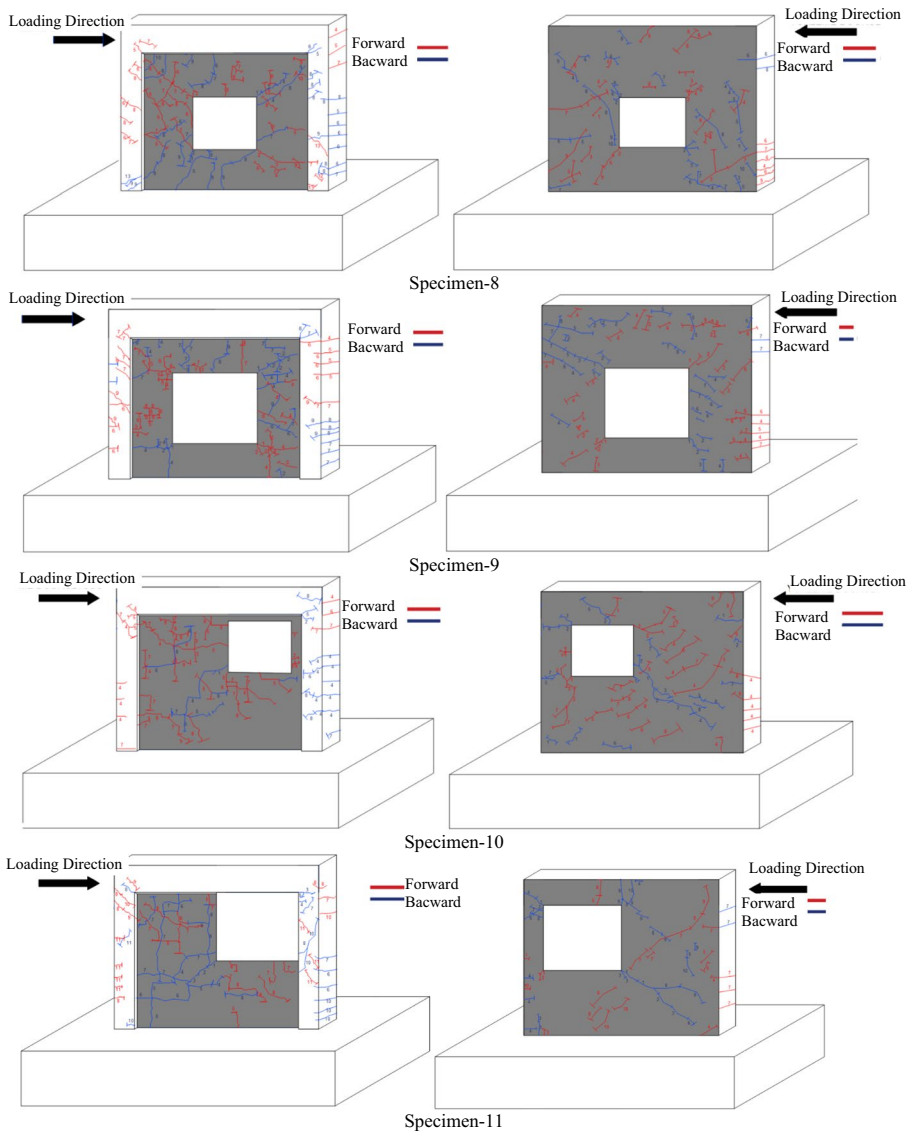


Fig. 10 Crack distributions of strengthened specimens with openings

the horizontal earthquake load carrying capacity more efficiently. The reinforced stucco layer used in the strengthening technique developed within the scope of the study took the horizontal earthquake load through environmental anchors placed on the RC frame and transferred it to the entire masonry infill wall through "L" shaped anchors placed on the masonry infill wall surface. It prevented the damage from being localized in one area with the cracks that occurred in the infill wall due to the horizontal earthquake load and ensured that it was dispersed. When the crack distributions were examined, it was seen that in the Specimen-8 and Specimen-9, where the opening was located in the middle of the infill

wall, the infill wall was divided into two wing walls and the crack distributions developed in such a way that two different independent diagonal bars were formed on the wing walls on both sides of the opening. However, as stated before, the strengthening technique developed prevented the cracks from concentrating in the diagonal directions of the wing infill wall and enabled them to be distributed over the entire infill wall surface, as seen in the figures. In Specimen 10 and Specimen 11, where the openings are located at the corner of the infill wall, it can be seen that crack distributions occur in diagonal directions and a single diagonal bar pair is formed in the infill wall sections that remain as a single piece in the sections where there is no opening in the infill walls. However, it was observed that the applied strengthening method prevented the cracks from localizing in the diagonal direction and allowed them to spread over the entire infill wall. An important difference in the crack distributions occurring in the specimens where the opening is located at the corner of the infill wall is the occurrence of short column behavior in the RC frame column located next to the opening and the formation of many bending and shear cracks in the column.

The strengthening method developed within the scope of the study completely changed the failure mechanism that occurred under the effect of horizontal earthquake loading in the RC frame specimens with masonry infill walls and distributed the damage by preventing the local crushing damage occurring at the diagonal strut ends of the infill wall and ensuring that the entire infill wall effectively took a share of the horizontal earthquake force. This change in the failure mechanism caused by the developed strengthening method has partially changed the sudden brittle fracture mechanism.

3.4 Stiffness and energy dissipation capacity changing behavior

When Fig. 11 is examined, it has been shown that the applied strengthening technique has not only a positive effect on the initial stiffness but also that the decrease in stiffness due to

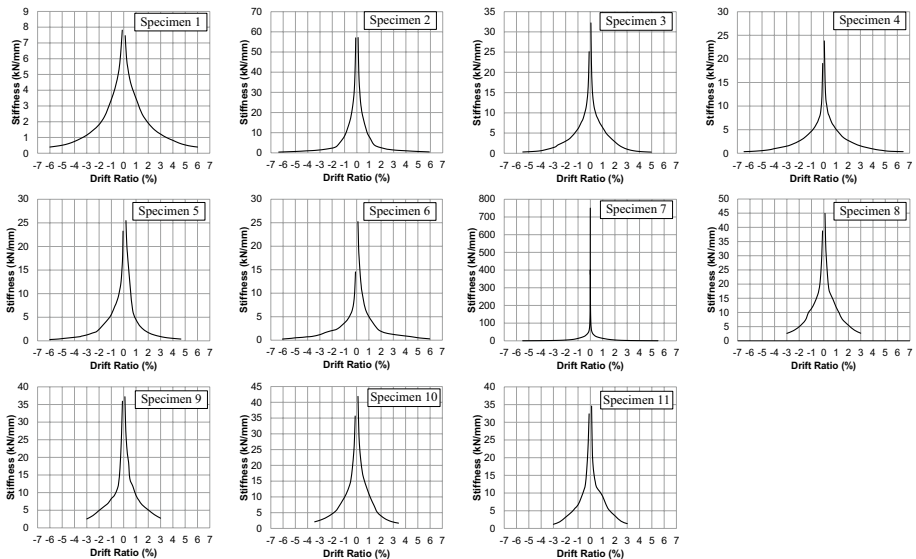


Fig. 11 Variation graphs of the stiffness of the specimens according to the story drift ratio

the increase in the story drift ratios of the specimens is limited by the applied strengthening method. The stiffness values decreased more slowly with the increase in the story drifts in the specimens to which the strengthening technique was applied. With the same approach, in addition to the total cumulative energy dissipation capacities of the specimens given in Table 4, the energy dissipation capacities of the specimens change with increasing displacement values, as presented graphically in Fig. 12. The normalized displacement values for each cycle were calculated by dividing the energy dissipation capacities of the specimens calculated in each cycle by 33 mm displacement, corresponding to a 1.0% story drift ratio of the maximum displacement value achieved in the cycle. The displacement values of the specimens at the maximum load level reached in each loading cycle were normalized by proportioning them to the 33 mm displacement value corresponding to the 1.0% story drift ratio value. The main reason for using 1.0% story drift ratio and the corresponding 33 mm displacement value in this normalization process is that this value is included in the regulations as the severe damage limit for RC frame type structures (European Committee for Standardization 2004). In the graph presented in Fig. 12, the normalized displacement values of the specimens on the x-axis are summed up, and the cumulative normalized displacement value is obtained. Each cycle's energy dissipation values are summed up on the Y axis, and the cumulative energy dissipation capacity is obtained. When the graphs presented in Fig. 12 are examined, it has been shown that the applied strengthening technique increases the energy dissipation capacity of the specimens for each cycle. The increase in the energy dissipation capacity of the specimens continued starting from very low story displacement values, and the strengthened specimens continued the increasing trend in their energy dissipation capacities in each cycle.

The strengthening method recommended within the scope of this study is recommended for structures with inadequate earthquake performance, that do not have sufficient horizontal earthquake load carrying capacity and rigidity, that have RC frame bearing systems that have many fundamental errors in their design, and that are likely to completely collapse or be severely damaged in the event of an earthquake. As stated in the article, a RC frame

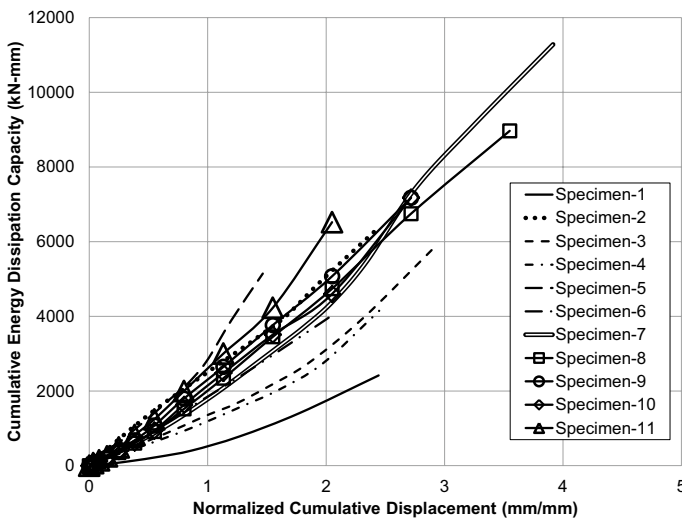


Fig. 12 Graphs of cumulative energy dissipation capacities of specimens by normalized cumulative displacement

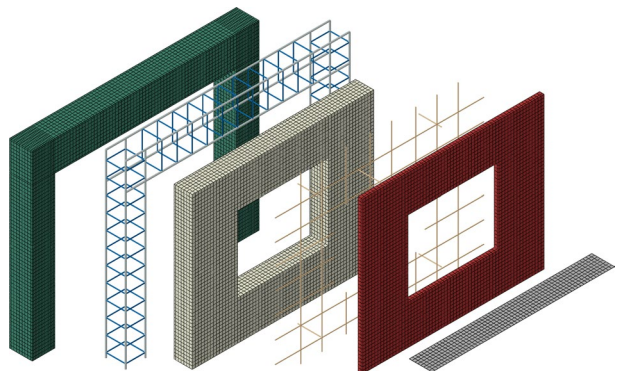
in which the strengthening was applied had design errors such as strong beam and weak column connections, insufficiency of shear reinforcement in columns and beams, and lack of shear reinforcement density in column-beam connection nodes. In this type of frame, it is a bearing system that may collapse by forming a column mechanism under the influence of horizontal earthquake loads, its earthquake performance is extremely inadequate, and its structural bearing system ultimate load capacity and rigidity are very inadequate. Since the earthquake performance of a RC frame with these features is insufficient, its energy dissipation capacity and ductility will be extremely low. Due to the selection of this type of RC frame, the first aim in the strengthening method applied is to significantly increase the bearing capacity and rigidity of the structural system with the strengthening performed. Of course, while the bearing capacity and rigidity are increased with the strengthening method applied, it is important that the energy dissipation capacity and ductility are not negatively affected. However, in a system whose bearing capacity and rigidity are very insufficient, it is necessary to first improve these properties, limit the story drift ratios of the building, and prevent it from collapsing or receiving severe damage due to excessive deformations. With the strengthening method proposed in this study, the bearing capacity and initial stiffness values of the RC frame bearing system with masonry infill walls, which has many design errors and insufficient earthquake performance as stated above, were increased by an average of 83% and 226%, respectively. In addition, with the proposed strengthening method, although there was a 38% decrease in the ductility ratio, the energy dissipation capacity of the bearing system was increased by an extremely high rate of 62% on average. When these results are evaluated, it is thought that the proposed strengthening technique will be effective and successful in increasing the earthquake performance of the building if the results are generalized and applied to a real building consisting of RC frames with such structural design errors (Angelis and Pecce 2020).

4 Numerical study

Experimental studies on strengthened masonry-infilled RC frames are limited due to their cost and time consumption. The method developed within the scope of this study is a strengthening method and was developed for the strengthening of undamaged structures that are likely to be damaged in an earthquake. It should be kept in mind that a separate experimental study should be carried out on the extent to which a similar method can be successful for retrofitting damaged structures. The developed method is proposed to strengthen undamaged structures with insufficient earthquake resistance. To account for changes in the parameters, such as the opening sizes and positions, the experimental study produced 11 different specimens. This section of the study provides details on the numerical models that were developed. It explains variables like contact properties, boundary conditions, and loadings. The results of the experimental study and computer analysis were compared. The numerical part of the study used ABAQUS/Explicit finite element software. When the literature was examined, it was seen that the number of studies presenting comprehensive numerical analysis models analyzing the behavior of RC frames with masonry infill walls with openings under the influence of earthquake loading was extremely limited (Akhoundi et al. 2016; Flippou et al. 2023; Milijaš et al. 2023). No study has been found in the literature examining the numerical analysis of RC frames masonry infilled walls with openings strengthened with the innovative strengthening method examined within the scope of this study.

Following the geometrical dimensions of 11 test specimens, finite element models were created. The models' concrete, masonry, and stucco layers were created using C3D8 elements. This cube-shaped, eight-node linear brick element has eight edges and eight corner nodes (Akhoundi et al. 2016). T3D2 elements are used to model the reinforcements. This element refers to a 2-node linear triangular element, which is a triangular-shaped element with two corner nodes and three edges (Smith 2009). R3D4 (4-node 3-D bilinear rigid quadrilateral) elements are also used to model the rigid surface area that represents the top of the foundation. The finite element model and reinforcement information in the assembly created for Specimen 9 are shown in Fig. 13. The reinforced concrete frame is the green element in this assembly. The frame element's reinforcements can be seen right next to it. The masonry, the stucco layer's reinforcement, and the stucco layer are shown. On the far right is the rigid surface element used to model the contact between the foundation and the elements on it. The end of the stucco layer reinforcement foundation side, the rigid surface element, and the bottom of the column are all modeled as fixed. Translational and rotational freedoms are restrained. While the numerical analysis models of the specimens were being created, the foundation beam parts of the RC frames were not modeled in order to reduce the size of the model and save computer time. It is thought that the RC frames of the specimens behave in a way that can be considered as fixed supports in the lower parts where they meet the foundation beam. For this reason, the surface shown as a gray surface on the far right in Fig. 13 is defined as a fixed support and all freedoms on this surface are restrained. All components such as the concrete volume of the RC frame, reinforcements, masonry infill wall volume, reinforcement layer added to the infill wall and stucco layer volume, which constitute the specimens, were coupled to this fixed surface. The model's top surface was used to load uniformly. As an example, the boundary conditions, contact surfaces, and loading surfaces used in the finite element model are given in Fig. 14 for the Specimen 9 test element. A suitable mesh size was determined by testing various mesh sizes on the model. Within the scope of the study, sensitivity analysis was performed to select the appropriate finite element mesh sizes. For the analyzes made for Specimen-9, as an example, the graph showing the variation of the story displacement value according to the selected element size is given in Fig. 15. When this graph was examined, it was seen that the most suitable mesh size was 20 mm. For the solid infill wall model, there are 22,410 finite elements in the reinforced concrete frame, 21,000 in the brick wall, and 6000 in the stucco layer. Thus, there are 51,293 elements in the model, including 49,410

Fig. 13 Specimen 9 element mesh, part assembly



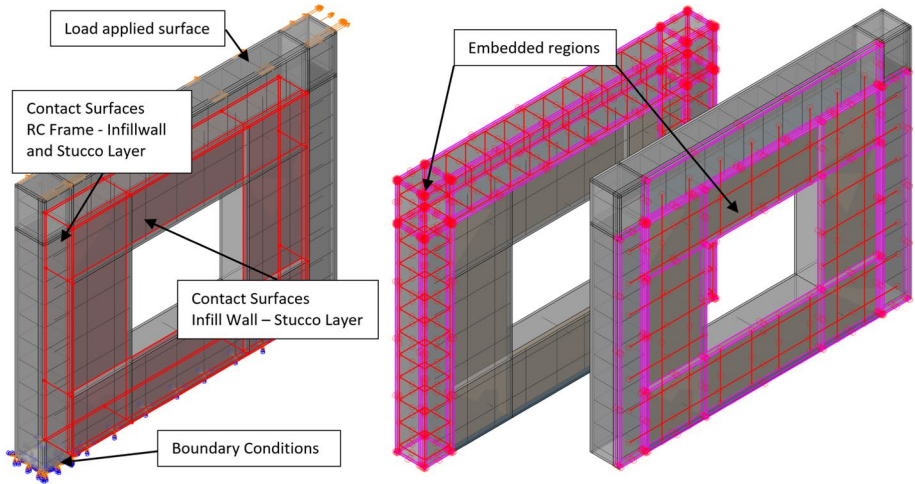
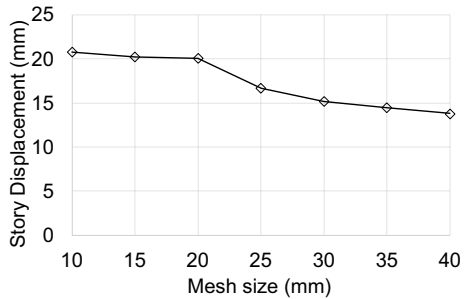


Fig. 14 Specimen 9 contact surfaces, load and boundary conditions, and embedded regions

Fig. 15 Specimen 9 sensitivity analysis graph for determining the finite element mesh size



linear hexahedral elements of type C3D8, 1403 linear line elements of type T3D2, and 480 linear quadrilateral elements of type R3D4.

Cyclic loading was performed in the lab experiment. But considering the analysis time, only a one-way pushover analysis was carried out in the numerical study. Using a standard solver does not offer an effective solution when material degradation or failure, such as concrete cracking, will result in a discontinuity in the solution. So, Abaqus/Explicit was used for numerical analysis. An approach to mathematically integrating the equations of motion through time is known as explicit dynamics. Nonlinear, quasi-static analysis can be analyzed using explicit solvers. When a horizontal load is applied, shear and tensile forces develop on the surface between the reinforced concrete frame and the infill wall. Usually, the damage starts on this contact surface. After the surface is damaged, friction force can transfer the load. In the numerical analysis model carried out using the ABAQUS finite element software presented within the scope of the study, all components forming the experimental elements were modeled with the micro modeling approach in the geometry and in the most detailed way possible, as they were actually produced. The masonry infill wall within the RC frame was not modeled with a diagonal bar, but was modeled as a separate volume in the geometry in which it was

actually produced. As a result of modeling the components that make up the specimens as separate volumes and continuous environments, the contact surfaces of these separate continuous environments must also be modeled and some parameters must be defined for load transfer to these contact surfaces. Likewise, in some continuous environments such as reinforcement, it was necessary to model them as embedded in other volumes and to define some parameters in this regard. The contact surfaces and embedded volumes in the specimens are given in Fig. 14 for the Specimen-9 selected as an example. It has been stated that damage begins at the interface of the RC frame and masonry infill wall due to the loading applied to the RC frame, and then, after damage occurs on the surface, the loading continues to be transferred only by friction. This is the approach used on the contact surface between the RC frame and the masonry infill wall. In their study, Motovali et al. modeled the contact surface with the cohesive contact surface (Motovali et al. 2018). Abaqus traction–separation behavior is initially linear elastic. The elastic behavior is written in an elastic structural matrix that relates the nominal stresses along the interface to the nominal stresses (Akhoundi et al. 2016). In this Eq. 1, coupling effects are not considered.

$$t = \begin{Bmatrix} t_n \\ t_s \\ t_t \end{Bmatrix} = \begin{Bmatrix} K_{nn} & 0 & 0 \\ 0 & K_{ss} & 0 \\ 0 & 0 & K_{tt} \end{Bmatrix} = k\delta \tag{1}$$

In this place t_n = normal traction, t_s and t_t = shear tractions, δ = separation vector.

The traction–separation laws in ABAQUS are divided into energy-based criteria for damage evolution and stress and strain-based criteria for damage initiation. When a quadratic interaction function involving the nominal stress ratios (as defined in the expression below) reaches a value of 1, the damage is assumed to have started (Eq. 2). The traction–separation laws graph used in the study is given in Fig. 16 (Debnath et al. 2023; Campilho et al. 2008).

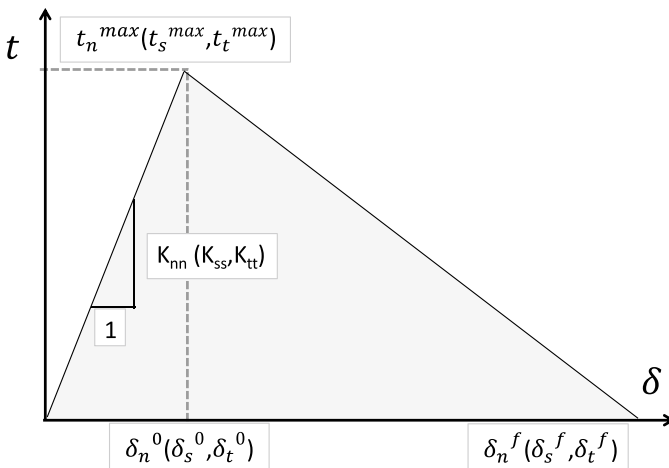


Fig. 16 Traction–separation response

Table 5 Cohesive contact behavior between masonry and concrete materials (Smith 2009)

Description	Value
Tangential behavior	0.57
Normal behavior	Hard contact
Cohesive behavior	
Traction separation behavior	
Stiffness coefficients	
K_{nn}	11 MN/m
K_{ss}	11 MN/m
K_{tt}	11 MN/m
Damage	
Initiation	
Normal only	0.1 MPa
Shear 1 only	0.15 MPa
Shear 2 only	0.15 MPa
Evolution	
Total/plastic displacement	1 mm
Exponential parameter	10

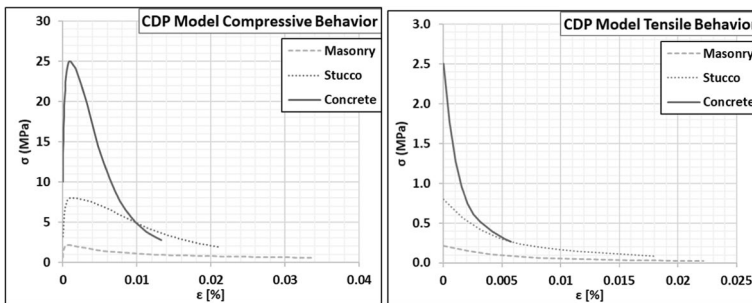


Fig. 17 Stress–strain curves for CDP models

$$\left\{ \frac{t_n}{t_n^{\max}} \right\}^2 + \left\{ \frac{t_s}{t_s^{\max}} \right\}^2 + \left\{ \frac{t_t}{t_t^{\max}} \right\}^2 = 1 \tag{2}$$

When the corresponding damage initiation criterion is reached, the cohesive stiffness degrades at a rate determined by the damage evolution law. Evolution based on the effective displacement approach is used in the model (Smith 2009). The data are shown in Table 5.

Concrete is a brittle material with nonlinear properties which can be defined by the concrete damage plasticity (CDP) model. Other concrete constitutive models using the smeared crack method are available in the ABAQUS material library (Hafezolghorani et al. 2017). The concrete damaged plasticity model’s main objective is to accurately predict how concrete structures behave under cyclic and dynamic loading. The model can analyze other quasi-brittle materials, including masonry, mortar, and rock. Borah et al. (Borah et al. 2020) used the CDP method to model the masonry wall with the macro modeling method

Table 6 Summary of CDP parameters

Description	Concrete	Masonry	Stucco	Unit	Source/Reference
Elastic modulus	25,196	1200.00	15,443.10	MPa	Calculated
Poisson ratio	0.2	0.15	0.20	–	Calculated
Density	2.4	2.0	2.4	t/m ³	Experiment
Dilation angle	40°	20°	48°	degree	Calibrated/Borah et al. (2020)
Eccentricity	0.10	0.10	0.10		Calibrated
fb0/fc0	1.16	1.16	1.16		Calibrated
K	0.5	0.75	0.67		Calibrated
Viscosity parameter	0.0025	0.001	0.002		Calibrated
Ultimate compression strength	25	2.16	8.00	MPa	Experiment
Maximum tensile stress	2.5	0.216	0.8	MPa	Calibrated

in the study. Material models created in masonry, stucco, and concrete elements are shown in Fig. 17. The values obtained from the material tests and the parameters calibrated to match the test results are shown in Table 6. Rebars are modeled as discrete elements. This way, the reinforcing truss structure is fully embedded in the reinforced concrete elements. The anchors between the stucco layer and the masonry infill wall are also perfectly bonded. According to the information gleaned from the test results, the reinforcement properties used in the models were modeled as bilinear material, and these values are shown in Table 7.

There are many theories about the damaged model in a finite element method (FEM) analysis reported in the literature. Among the damaged models, the concrete damaged plasticity (CDP) model is considered the most reliable use in simulation. Based on this model, by using many other techniques, many damaged models have been proposed. Most improved techniques are based on developing a new stress–strain relationship in both compression and tension or proposing a novel function to calculate damaged parameters in compression (d_c) and tension (d_t). Lubliner et al. (1989) was proposed a novel constitutive model lied on plasticity theory for the non-linear analysis of concrete. A new yield criterion was presented which accounts for both elastic and plastic stiffness degradations effects. Comparing results between numerical simulation and experimental methods showed that the model responded well to applications. Carol et al. (2001) was presented as a formulation for tensile damage. One of the important advantages of the model is that closed-form solutions are possible for some loading cases. Damaged models which are based on presenting a novel curve of stress–strain in three dimensions stress can find in reports of. Ahmed et al. (2020) were proposed a damaged model based on the novel stress accounting for damaged shear. The new stress makes further decompose tensile and compressive

Table 7 Mechanical properties of steels

	E (MPa)	Poisson ratio	Density (t/m ³)	Yield Strength (MPa)	Ultimate Strength (MPa)
φ6 Rebars	210,000	0.30	7.90	330	410
> φ6 Rebars	205,000	0.30	7.90	544	585
Mesh	207,000	0.30	7.90	576	615
Source	Experiment	Calculated	Experiment	Experiment	Experiment

parts into pure biaxial shear and pure tensile/compressive biaxial stresses. The theory of Lubliner theory (Lubliner et al. 1989) was employed to develop a new method to modify the damaged concrete model by Lee and Fenves (1998). Thus, this proposed model was accounted for confinement having a uniform and non-uniform condition. Jason et al. (2006) introduced the new function to calculate the damaged elastic–plastic. This model has overcome the limitations of pure elastic–plastic damage in the case un-loading phase. Grassl et al. (2011) were used the combination of damage mechanics and plasticity flow to investigate the concrete structure under dynamic loading conditions, etc. The concrete damaged plasticity model (CDP) in combination with the tensile damage variable (d_t) and compressive damage variable (d_c) were followed by Birtel and Mark (2006).

Table 8 presents a summary of the results of the numerical study. The test results on the concrete samples produced relatively low standard deviations for the compressive strengths. Analyses were carried out using the average of these values to provide a general statement. The pushover analysis results were compared to a portion of the cyclic load–displacement envelope curves obtained from laboratory experiments in one direction. In Fig. 18, this comparison is displayed. As a result, it was discovered that the results were largely consistent. Figure 19 illustrates failure patterns under ultimate load consistent with symmetrical models. The change of direction of the load affected the crack propagation and caused the differentiation of the resulting mechanism. However, this situation did not create a significant difference when compared in terms of consumed energy. In the experimental study, the loading history given in Fig. 6 is applied, which is repeated reversibly on the specimens in both directions. However, in the numerical analysis study carried out within the scope of the study, a pushover analysis was performed by applying a loading in one direction to the analysis models. For this reason, the damage distributions given in Fig. 19 can only be compared with the damage distributions obtained from the experimental study with an aspect obtained in the forward loading steps. In the experimental study, it was impossible to compare the damage and cracks occurring in the backward cycles in the other direction with the crack distributions obtained due to the numerical analysis. Since the static push over analysis was carried out by applying force in one direction in the numerical analysis study, it was observed that there were diagonal cracks in one direction in the specimens, depending on the applied loading direction, and sections where crushing occurred in the

Table 8 Comparison of experimental and finite element analysis results

Spec. No	Ultimate load (kN)			Displacement at ultimate load (mm)		
	Experiment	FEM	Ratio	Experiment	FEM	Ratio
1	42.00	31.91	0.76	22.00	12.10	0.55
2	94.00	69.97	0.74	9.04	8.20	0.91
3	72.15	68.62	0.95	12.99	8.80	0.68
4	59.43	59.02	0.99	12.93	8.10	0.63
5	64.92	59.90	0.92	3.84	9.80	2.55
6	53.20	51.84	0.97	8.82	13.30	1.51
7	155.00	174.10	1.12	10.27	10.90	1.06
8	135.12	95.39	0.71	13.75	17.35	1.26
9	112.01	83.44	0.74	22.00	20.10	0.91
10	121.05	94.35	0.78	12.54	14.00	1.12
11	99.88	95.30	0.95	11.00	14.40	1.31

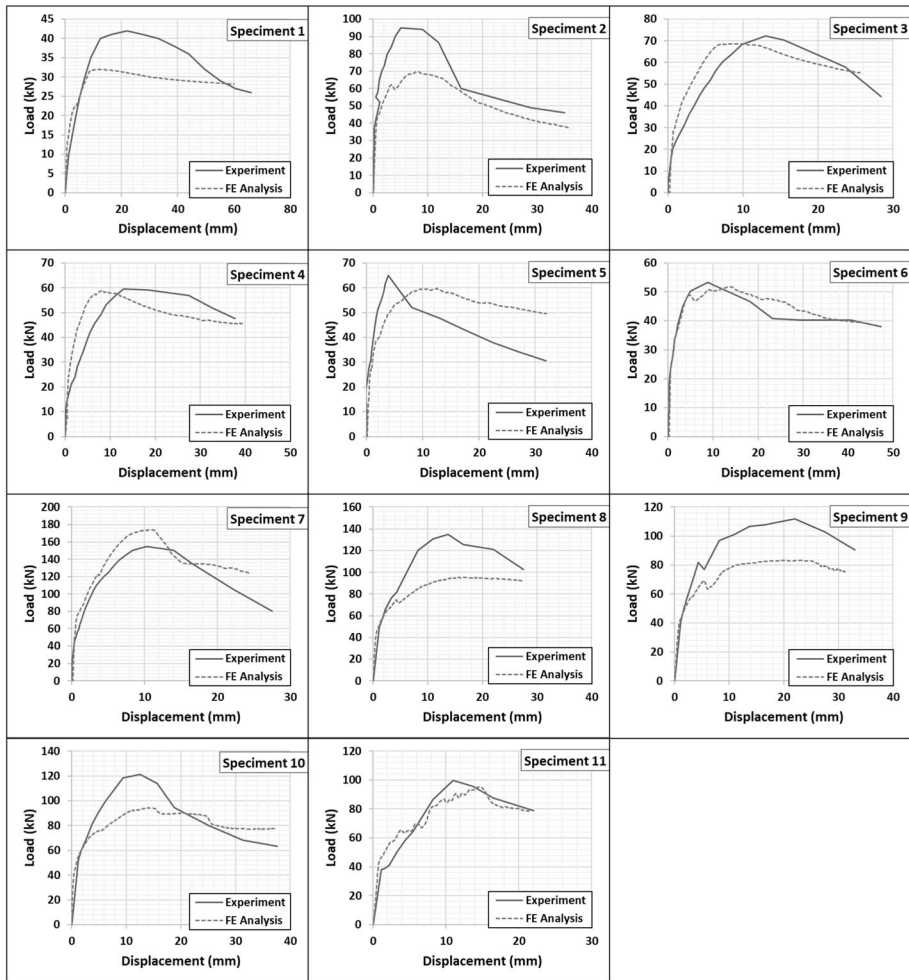


Fig. 18 Comparison of experimental and numerical load–displacement graphs

end regions of the diagonal bars formed in the masonry infill walls, depending on the loading direction. When evaluated from this perspective, it was not possible to compare the damage distribution obtained as a result of the experimental study with the damage distribution obtained as a result of numerical analysis. However, although the cracks and damage distribution resulting from the effect of horizontal force applied in one direction are obtained as a result of the numerical analysis, it is seen that there is a significant similarity and harmony between the experimental damage distribution and the numerical analysis damage distribution. It is seen that the damage distribution obtained from the numerical analysis and the experimental damage distribution are concentrated at the same points, the cracks occur and progress in the same direction, and the failure mechanisms are generally compatible.

As a result of the numerical analysis, it is seen that the initial stiffness values and general load–displacement behavior of all specimens have been determined quite successfully

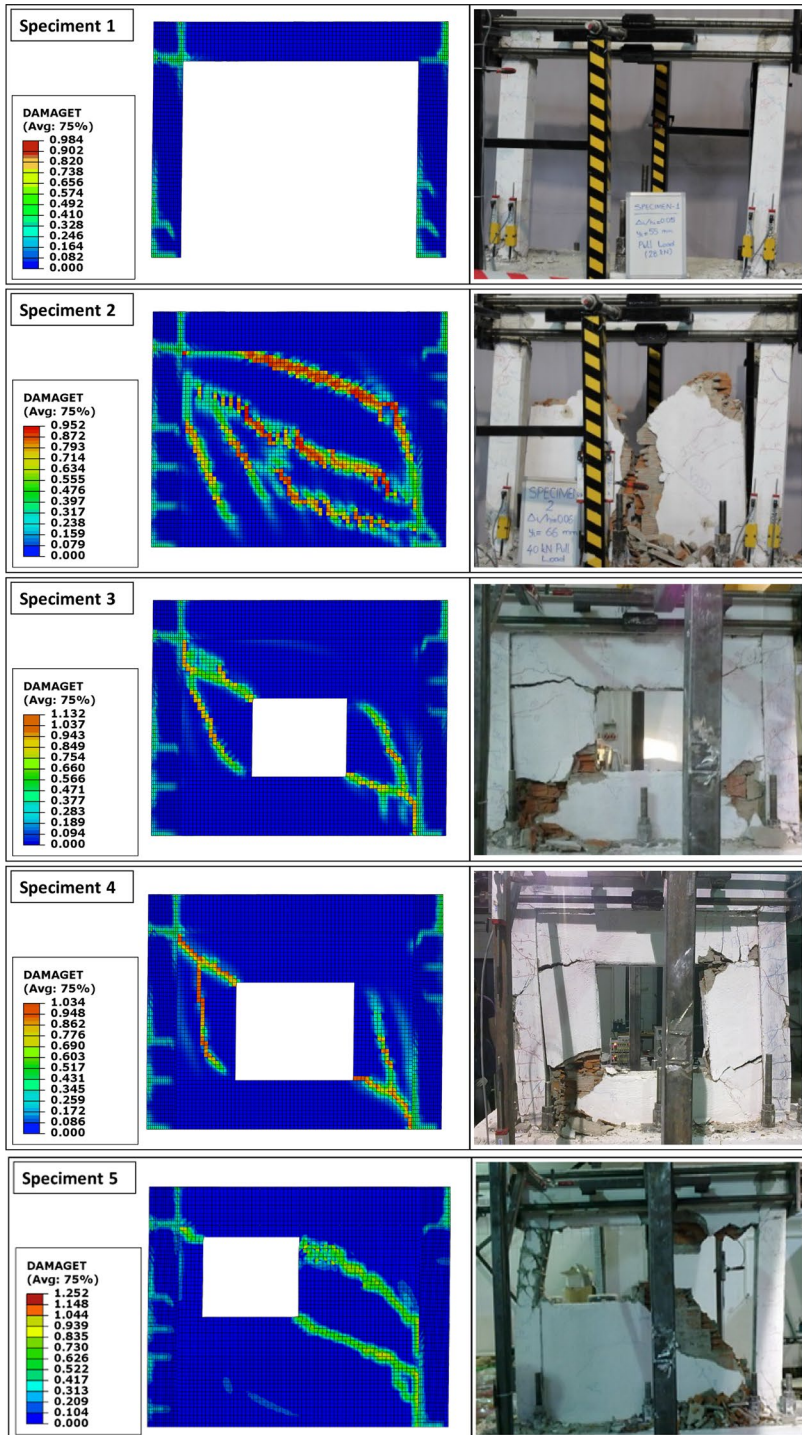


Fig. 19 Comparison of tensile damage on ultimate load and experimental damage distribution

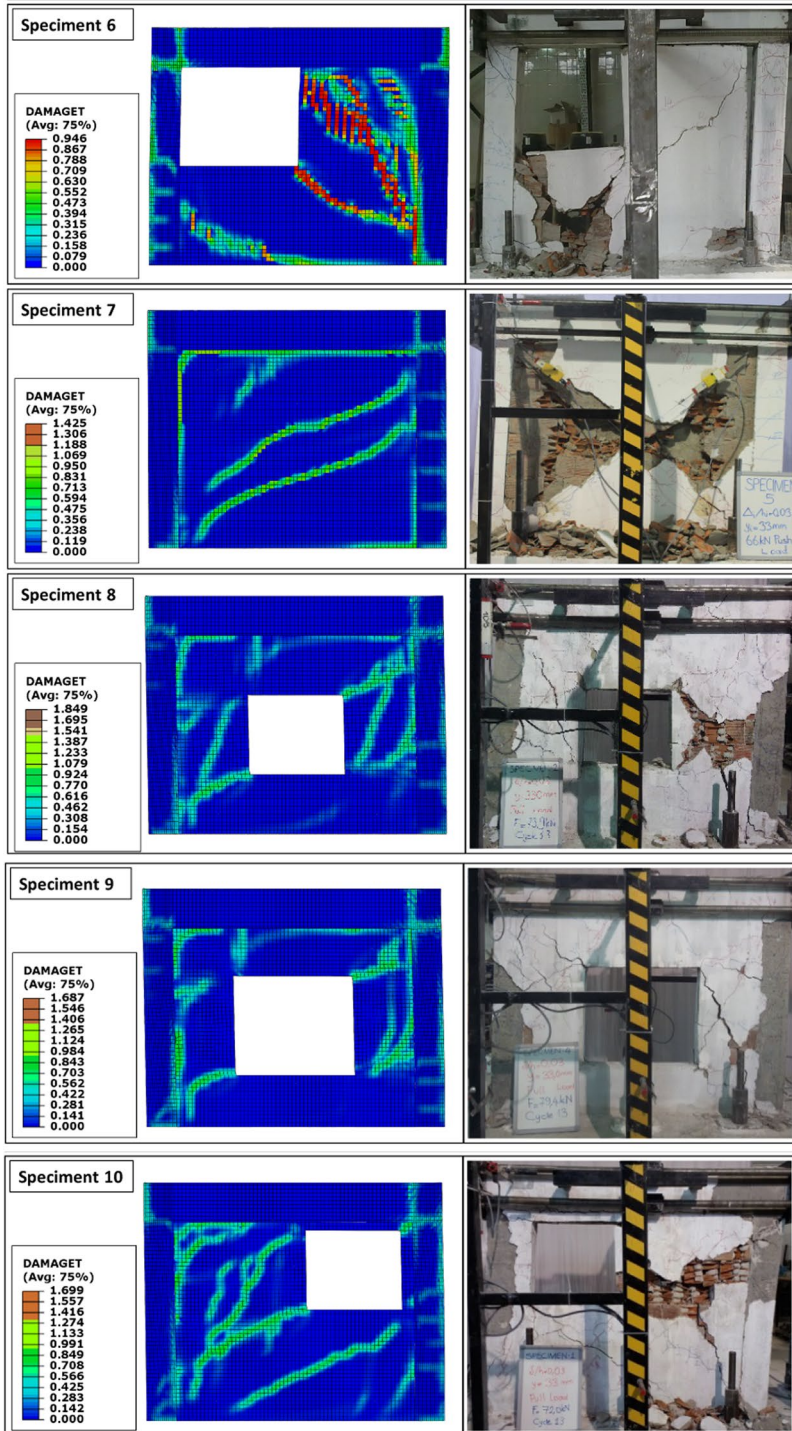


Fig. 19 (continued)

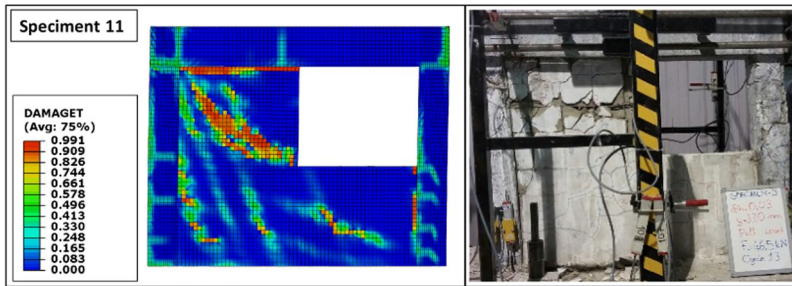


Fig. 19 (continued)

and in accordance with the experimental load–displacement graphs. Especially in the decreasing capacity section after the point where the ultimate load capacity is reached, where the decrease in ultimate capacity occurs from the numerical analysis model, a very compatible and successful simulation has been obtained with the experimental results. However, in Specimen 8, 9, and 10 where the strengthening method was applied, the ultimate load capacity was calculated lower than the experimental results in the numerical analysis. It is thought that the main reason why the capacity values calculated as a result of numerical analysis are lower than the experimental capacity is due to the fact that the damage parameters of the masonry and the stucco layer added for strengthening purposes are not fully known. In the numerical model, CDP material model was used for all three materials: concrete, masonry and stucco layer. It is possible to find a large number of studies and commonly preferred values in the literature regarding the parameters that can be used for concrete in the CDP material model. However, no study has been found in the literature regarding the CDP model parameters that can be used for the masonry and stucco layer added for strengthening. It is thought that the compatibility of the numerical analysis results with the experimental results can be increased for Specimen 8, 9 and 10, which were strengthened by performing a parametric study regarding these values.

5 Conclusions

This study aims to develop a strengthening technique that can be applied quickly and easily, does not require complicated labor, and is low in cost, all while causing minimal disruption to the residents. It is aimed to examine the effects of the openings left in the masonry infill walls for the passage of the door, window, and installation systems on the strengthening technique in the structures with the RC frame-type bearing system with insufficient seismic performance. Except for the RC bare frame and the RC frame system with solid masonry infill walls, the reference specimens and two groups with openings were produced in the study. One of these groups contains specimens that have been strengthened using the research's recommended reinforced stucco layer addition method, while the other contains specimens that have not been strengthened. These experiments determined how the proposed strengthening method improves overall load–displacement behavior and seismic performance. Furthermore, nonlinear finite element models of the specimens were simulated using ABAQUS finite element software, and the numerical analysis results were compared and interpreted with the experimental results. The results obtained are shown below.

- It has been observed that the openings left in RC frames with masonry infill walls harm the frames' behavior when subjected to earthquake loading. The openings in the masonry infill wall reduced the ultimate load capacity, initial stiffness, displacement ductility ratio, and energy dissipation capacity values. The increase in the dimension of the opening in the masonry infill walls had a significant negative impact on the general load–displacement behavior and performance of the masonry-infilled RC frames under earthquake loading. The increase in the dimensions of the opening in the masonry infill wall caused a decrease in the ultimate load capacity, initial stiffness, displacement ductility ratio, and energy dissipation capacity values.
- The fact that the openings in the masonry infill walls are located in the corners close to the frame had a larger negative impact on the behavior under the effect of earthquake loading than the fact that they are in the middle of the frame.
- The proximity of the opening to the corner of the masonry infill wall caused a decrease in the ultimate load capacity, initial stiffness, displacement ductility ratio, and energy dissipation capacity values. Furthermore, the proximity of the opening to the corner resulted in short column behavior and shear cracks in the RC frame column.
- The study's recommended masonry-infilled RC frames with openings by adding a rebar-reinforced stucco layer strengthening approach improved the overall load–displacement behavior and performance under seismic loading. The ultimate load capacity, initial stiffness, and energy dissipation capacities of RC frames with masonry-infilled increased significantly. The negative effect of the applied strengthening method on displacement ductility ratios was also limited. When the proposed strengthening method for the masonry-infilled RC frame with an opening is compared to the RC frame with masonry infill wall without openings in terms of ultimate load and energy dissipation capacities, it has caught up to and even surpassed the performance of the RC frame with masonry infill wall without openings.
- However, when evaluated in terms of initial stiffness and displacement ductility ratios, the strengthened specimens with an opening masonry infill wall could not reach the performance level of the solid infill walls.
- The study's recommended strengthening approach also positively affected the failure mechanisms of masonry-infilled RC frames. The reinforced stucco layer ensured that the horizontal earthquake loading transmitted from the frame to the infill wall was distributed evenly across the entire infill wall. Local corner crushing in the infill wall and local shear cracks in the diagonal direction is restricted. The shear cracks spread throughout the infill wall, and the reinforced stucco layer added to its bearing strength. Furthermore, the strengthening method reduced the shear damage in the column caused by the short column mechanism that occurs when the opening is in the corner.
- Within the scope of the study, suggested masonry-infilled RC frames with openings by adding rebar-reinforced stucco layer strengthening technique that can be applied in considerably less time, with less work, less disturbance to building occupants, and at a very cheap cost compared to existing traditional techniques.
- In the experimental study carried out within the scope of this study, the RC frame with masonry infill walls was tested in the plane of the specimens under the effect of horizontal earthquake loads. The developed strengthening method aims to increase the performance of the infilled frame specimens under the effect of horizontal earthquake loading within their planes. For this reason, the out-of-plane behavior of RC frames with masonry infill walls is out of the scope of this study. In this regard, no measurements were taken from the specimens, and a type of loading to examine their out-of-plane behavior was not applied to the specimens. However, when the developed reinforcement technique is examined in

terms of the out-of-plane behavior of RC frames with masonry infill walls, it is thought that it will give positive results and improve behavior in this respect. As it is known, when the out-of-plane behavior under the effect of earthquake loading in RC frames with masonry infill walls without strengthening is evaluated, it is seen that the weak connection of the RC frame and the masonry infill wall affects the performance negatively. RC frames with infill walls without strengthening collapsed out of their planes due to the separation of the infill wall from the RC frame at very low load levels and story drift ratios. It is thought that the strengthened stucco layer added on the masonry infill wall in the developed strengthening technique will be attached to both the infill wall and the RC frame with a large number of anchors, which will prevent the infill wall from separating from the RC frame to a large extent. In addition, the strengthened stucco layer is thought to ensure that the infill wall behaves as a whole and like a reinforced plate that tries to bend out of its plane. However, all this interpretation is based only on the authors' predictions, and during the tests carried out, no loading to test the out-of-plane behavior was applied to the specimens, and no experimental data were obtained by taking any deformation measurements. As stated above, the specimens in this study were tested by loading them in their planes, and the developed strengthening technique was evaluated in terms of how much it improved the performance of RC frames with masonry infill walls under the effect of earthquake loads in their planes.

- With the numerical analysis performed, the general load–displacement behavior of all experimental specimens tested in the experimental program, initial stiffnesses, and the decrease in capacity after reaching the ultimate load capacity were obtained successfully and in accordance with the experimental results. However, the ultimate load capacities calculated by numerical analysis in the strengthened specimens were determined to be smaller than the experimental capacity values.
- It was thought that the main reason why the ultimate load capacity values calculated from the numerical analyzes carried out for the strengthened specimens were lower than the experimental values was due to the CDP model parameters used for masonry and stucco layer, and a comprehensive study should be carried out to determine these parameters.

Funding Open access funding provided by the Scientific and Technological Research Council of Türkiye (TÜBİTAK). There is no funding in this article.

Declarations

Conflict of interest All of the authors declare that he/she has no conflict of interest.

Human and Animal rights This article does not contain any studies with animals performed by any of the authors. This article does not contain any studies with human participants or animals performed by any of the authors.

Open Access This article is licensed under a Creative Commons Attribution 4.0 International License, which permits use, sharing, adaptation, distribution and reproduction in any medium or format, as long as you give appropriate credit to the original author(s) and the source, provide a link to the Creative Commons licence, and indicate if changes were made. The images or other third party material in this article are included in the article's Creative Commons licence, unless indicated otherwise in a credit line to the material. If material is not included in the article's Creative Commons licence and your intended use is not permitted by statutory regulation or exceeds the permitted use, you will need to obtain permission directly from the copyright holder. To view a copy of this licence, visit <http://creativecommons.org/licenses/by/4.0/>.

References

- Ahani E, Mousavi MN, Ahani A, Kheirollahi M (2019) The effects of amount and location of openings on lateral behavior of masonry infilled RC frames. *KSCE J Civ Eng* 23:2175–2187. <https://doi.org/10.1007/s12205-019-0714-x>
- Ahmed B, Voyiadjis GZ, Park T (2020) Damaged plasticity model for concrete using scalar damage variables with a novel stress decomposition. *Int J Solids Struct* 191–192:56–75. <https://doi.org/10.1016/j.ijsolstr.2019.11.023>
- Akhoundi F, Lourenço PB, Vasconcelos G (2016) Numerically based proposals for the stiffness and strength of masonry infills with openings in reinforced concrete frames. *Earthq Eng Struct Dynam* 45(6):869–891. <https://doi.org/10.1002/eqe.2688>
- Altun S, Anil Ö, Kara ME, Kaya M (2008a) An experimental study on strengthening of masonry infilled R/C frames using diagonal CFRP strips. *Compos B Eng* 39(4):680–693. <https://doi.org/10.1016/j.compositesb.2007.06.001>
- Altun S, Anil Ö, Kara ME (2008b) Strengthening of R/C nonductile frames with R/C infills: an experimental study. *Cement Concre Compos* 30(7):612–621. <https://doi.org/10.1016/j.cemconcomp.2007.07.003>
- Altun S, Kuran F, Anil Ö, Kara ME (2008c) Rehabilitation of heavily earthquake damaged masonry buildings. *Struct Eng Mech* 30(6):651–664. <https://doi.org/10.12989/sem.2008.30.6.651>
- Altun S, Anil Ö, Koprman Y, Belgin Ç (2010) Strengthening masonry infill walls with reinforced plaster. *Proc Inst Civil Eng Struct Build* 163(SB5):331–342. <https://doi.org/10.1680/stbu.2010.163.5.331>
- Altun S, Anil Ö, Kara ME, Koprman Y (2012) Comparison of seismic performance of RC frames strengthened with four different techniques. *Adv Struct Eng* 15(2):343–357. <https://doi.org/10.1260/1369-4332.15.2.343>
- ACI374.1-05 (2005) Acceptance criteria for moment frames based on structural testing and commentary, vol 374.1-05, ed: American Concrete Institute
- Angiolilli M, Gregori A, Vailati M (2020) Lime-based mortar reinforced by randomly oriented short fibers for the retrofitting of the historical masonry structure. *Materials* 13(16):3462
- Anil Ö, Altun S (2007) An experimental study on reinforced concrete partially infilled frames. *Eng Struct* 29(3):449–460. <https://doi.org/10.1016/j.engstruct.2006.05.011>
- Birtel V, Mark P (2006) Parameterised finite element modelling of RC beam shear failure. *Abaqus User's Conference*, pp 95–108
- Borah B, Kaushik HB, Singhal V (2020) Finite element modelling of confined masonry wall under in-plane cyclic load. *IOP Conf Ser Mater Sci Eng* 936(1):012020
- Campilho RD, De Moura MFSF, Domingues JJMS (2008) Using a cohesive damage model to predict the tensile behaviour of CFRP single-strap repairs. *Int J Solids Struct* 45(5):1497–1512
- Carol I, Rizzi E, Willam K (2001) On the formulation of anisotropic elastic degradation. II. Generalized pseudo-Rankine model for tensile damage. *Int J Solids Struct* 38(4):519–546. doi [https://doi.org/10.1016/S0020-7683\(00\)00031-7](https://doi.org/10.1016/S0020-7683(00)00031-7)
- De Angelis A, Pecce MR (2020) The role of infill walls in the dynamic behavior and seismic upgrade of a reinforced concrete framed building. *Front Built Environ Sec Earthq Eng* 6. <https://doi.org/10.3389/fbuil.2020.590114>
- Debnath P, Dutta SC, Halder L et al (2023) Lateral behaviour of unreinforced masonry walls with different sizes and locations of opening and effect of strengthening measures: a computational approach. *Bull Earthq Eng*. <https://doi.org/10.1007/s10518-023-01798-5>
- EN 1998-1 (2004) Eurocode 8: design of structures for earthquake resistance—Part 1: general rules, seismic actions and rules for buildings, 2004, European Committee for Standardization
- Flippou CA, Nicholas CK, Christis ZC (2023) Numerical study of the seismic retrofitting of masonry-infilled RC frames with openings using TRM. *Earthq Eng Struct Dynam* 52:776–805. <https://doi.org/10.1002/eqe.3787>
- Grassl P, Nyström U, Rempling R, Gylltoft K (2011) A damage-plasticity model for the dynamic failure of concrete. In: *Proceedings of the 8th international conference structuring dynamic, EURO DYN 2011*, pp 3287–3294
- Hafezolzghorani M, Hejazi F, Ramin V, Jaafar MSB, Karimzadeh K (2017) Simplified damage plasticity model for concrete. *Struct Eng Int* 27(1):68–78. <https://doi.org/10.2749/101686616X1081>
- Jason L, Huerta A, Pijaudier-Cabot G, Ghavamian S (2006) An elastic plastic damage formulation for concrete: application to elementary tests and comparison with an isotropic damage model. *Comput Methods Appl Mech Eng* 195(52):7077–7092. <https://doi.org/10.1016/j.cma.2005.04.017>
- Kakaletsis DJ, Karayannis CG (2008) Influence of masonry strength and openings on infilled R/C frames under cycling loading. *J Earthq Eng* 12:197–221. <https://doi.org/10.1080/13632460701299138>

- Kaya F, Tekeli H, Anil Ö (2018) Experimental behavior of strengthening of masonry infilled reinforced concrete frames by adding rebar-reinforced stucco. *Struct Concr* 19(6):1792–1805. <https://doi.org/10.1002/suco.201700210>
- Khoshnoud HR, Marsono K (2016) Experimental study of masonry infill reinforced concrete frames with and without corner openings. *Struct Eng Mech* 57:641–656. <https://doi.org/10.12989/sem.2016.57.4.641>
- Koutas L, Bousias S, Triantafyllou T (2014) Seismic strengthening of masonry-infilled RC frames with TRM: experimental study. *J Compos Constr.* [https://doi.org/10.1061/\(ASCE\)CC.1943-5614.0000507.04014048](https://doi.org/10.1061/(ASCE)CC.1943-5614.0000507.04014048)
- Lee J, Fenves GL (1998) Plastic-damage model for cyclic loading of concrete structures. *J Eng Mech* 124(8):892–900. [https://doi.org/10.1061/\(asce\)0733-9399\(1998\)124:8\(892\)](https://doi.org/10.1061/(asce)0733-9399(1998)124:8(892))
- Lubliner J, Oliver J, Oller S, Onate E (1989) A plastic-damage model for concrete. *Int J Solids Struct* 25:299–326
- Makou G (2021) A new method of seismic retrofitting cost analysis and effectiveness for reinforced concrete structures. *Eng Struct* 246:113083. <https://doi.org/10.1016/j.engstruct.2021.113083>
- Mercuri M, Vailati M, Gregori A (2023) Lime-based mortar reinforced with randomly oriented polyvinyl-alcohol (PVA) fibers for strengthening historical masonry structures. *Dev Built Environ* 14:100152
- Milijaš A, Šakić B, Marinković M, Butenweg C, Gams M, Klinkel S (2023) RC frames with masonry infills with and without openings: experimental and numerical results. In: Papadrakakis M, Fragiadakis M (eds) *COMPADYN 2023, 9th ECCOMAS thematic conference on computational methods in structural dynamics and earthquake engineering*, Athens, 12–14 June 2023
- Mojsilović N (2022) Structural behavior of masonry walls with soft-layers: an overview of experimental work. *Current Perspectives and New Directions in Mechanics, Modelling and Design of Structural Systems 1928–1933*. CRC Press
- Motovali E, Mohammad S, Mohammadi M, Lourenco P (2018) Equivalent diagonal strut method for masonry walls in pinned connection and multi-bay steel frames. *J Seismol Earthq Eng* 19(4):299–311
- Sakr MA, El-Khoriby SR, Seleemah AA, Aboelnour MM, Osama B (2021) Experimental and numerical investigation on cyclic behavior of masonry infilled RC frames retrofitted with partially bonded CFRP strips. *Structures* 33:2238–2252. <https://doi.org/10.1016/j.istruc.2021.05.087>
- Sigmund V, Penava D (2013) Influence of openings, with and without confinement, on cyclic response of infilled R-C frames—an experimental study. *J Earthq Eng* 18:113–146. <https://doi.org/10.1080/13632469.2013.817362>
- Smith M (2009) *ABAQUS/standard user's manual, version 6.9*; Dassault Systèmes Simulia Corp., Providence, RI
- Vailati M, Mercuri M, Angiolilli M, Gregori A (2021) Natural-fibrous lime-based mortar for the rapid retrofitting of heritage masonry buildings. *Fibers* 9(11):68
- Vailati M, Gregori A, Mercuri M, Monti G (2023a) A non-intrusive seismic retrofitting technique for masonry infills based on bed-joint sliding. *J Build Eng* 69:106208
- Vailati M, Di Gangi G, Quaranta G (2023b) Thermo-mechanical characterization and hysteretic behavior identification of innovative plastic joint for masonry infills in reinforced concrete buildings. *J Build Eng* 65:105803
- Wang F (2023) Experimental research on seismic performance of masonry-infilled RC frames retrofitted by using fabric-reinforced cementitious matrix under in-plane cyclic loading. *Int J Concr Struct Mater* 17:31. <https://doi.org/10.1186/s40069-023-00594-4>
- Zhang C, Yu T, Chen Z, Huang W, Zhang S, Zhou Y, Lin Z (2022) Seismic behavior of novel low-damage precast infill walls with sliding joints for reinforced concrete frame. *Earthq Eng Struct Dynam* 51(15):3730–3754